Toward Wearable Multimodal Neuroimaging

An Interactive Qualifying Project
submitted to the faculty of

WORCESTER POLYTECHNIC INSTITUTE

In partial fulfillment of the requirements
for the Bachelor of Science

by

Prudence Lam
Jack Sullivan
Maceo Richards
Shane Stevens

Date: January 6, 2021

Advised by Professor Ali Yousefi and Professor Soroush Farzin

Statement of Authorship

This paper was written and compiled by Prudence Lam, Jack Sullivan, Maceo Richards, and Shane Stevens in partial fulfillment of our IQP. The table below lists an authorship statement for each section.

Section	Contributions
Introduction	Lead author: Prudence Editor: Jack
Background and Relevant Works	Lead author: Prudence Editor: Prudence
Market Research	Lead authors: Jack, Shane Editor: Prudence
System Architecture	Lead authors: Prudence, Shane, Jack Editors: All
Experimental Studies	Lead authors: Jack, Maceo Editor: Shane, Prudence
Experimental Results and Discussion	Lead authors: Jack, Maceo Editor: Jack
Conclusion	Lead author: Jack Editors: All
Miscellaneous	Structure taken from the CVPR 2018 template, cover page designed by Prudence

Contents

List of Figures

List of Tables

Abstract

EEG and other Brain-Computer Interfaces (BCI) are seeing increased use in cognitive neuroscience because of the powerful neuroimaging data they deliver. In particular, wearable neuroimaging technologies, or "wearables", have enabled prolonged, non-invasive recordings in motion-rich environments. Two techniques - electroencephalogram (EEG) and functional near-infrared spectroscopy (fNIRS) - have been widely commercialized due to being non-invasive and low-cost. However, limitations in their technology, namely variable signal quality and susceptibility to artefacts, have prevented them from reaching their full potential. This paper proposes an adhesive, EEG-fNIRS wearable patch as a solution to these limitations. As measures of electrical and hemodynamic responses of the brain, respectively, EEG and fNIRS possess complementary features shown to be capable of creating more robust features. The paper also presents the EEG analysis of three proof-of-concept experiments and the device's performance compared to baseline metrics provided by the DSI-24 EEG Headset.

1. Introduction

Robust characterizations of brain-behavior relationships are a long-standing goal in cognitive neuroscience. With the advent of *neuroimaging techniques*, specifically *functional neuroimaging*, cognitive models have pivoted from neuropsychological tests evaluating behavioral responses, to visualizations of the biological processes that underpin them [51, 63]. These techniques involve localizing cognitive processes spatially (e.g. with *functional magnetic resonance imaging* (fMRI) and *functional near-infrared spectroscopy* (fNIRS)) or temporally (e.g. with *electroencephalography* (EEG)).

In classical neuroimaging investigations, participants undertake a series of experiments that evoke activity in specific brain regions. Often, these experimental paradigms are contingent on the choice of imaging instrument. Such instruments can be obstructive, as in the case of large EEG headsets, or fixed, as with fMRI scanners [49]. Other experimental constraints include high equipment costs and lengthy set-up times. Recent developments in sensors and circuitry have led to a proliferation of wearable brain-sensing solutions for consumer use. These devices enable flexible, real-time monitoring of localized brain activity in non-specialist, motion rich environments.

Wearable EEG is perhaps by far the most established portable imaging technique. It has found applications in personalized health, such as sleep monitoring [47, 55, 23], stress analysis [5, 29], seizure detection [13], drowsiness detection [40, 42], and brain training (via neurofeedback) [15]. Other applications include emotion recognition [22], architectural and urban design [34], musical pleasure [17], and brain-computer interfaces (BCIs) [16]. Despite these successes, wearable EEG systems face several bottlenecks. Firstly, their signal quality is more variable than research-grade systems, particularly in dry electrodes (as opposed to gel-based systems) [27]. Secondly, their electrode density must be low for affordability and user comfort, but not enough to compromise source localization, signal quality, artefact rejection, referencing/re-referencing schemes [41]. An absence of sensors on vital regions can also generate significant information loss.

In this paper, we present a multimodal solution to overcome these challenges. Multimodal functional neuroimaging is the concurrent assessment of two or more complementary neurophysiological processes. Previous studies have successfully combined hemodynamic and electrical information using EEG and fMRI [6, 65]. However, fMRI's fixed location and high cost prevent it from being used outside a laboratory. For this reason, multimodal studies have expressed interest in fNIRS, a portable and cost-effective light-based technique. We hypothesize that because fNIRS and EEG have high spatial and temporal resolutions, respectively, one can compensate for information loss in the other.

Thus, the study's objectives are to:

- Provide a proof-of-concept of a portable EEG-fNIRS device.
- Evaluate the device against several experimental benchmarks
- Identify possible trajectories for generations of this device.

The organization of this paper closely follows our team's steps in achieving these objectives. Section 2 provides an overview of relevant research in the fields of cognitive neuroscience and modern BCI technology. Section 3 takes this technical background into market research, identifying various BCI products and evaluating them based on a value analysis. Section 4 outlines our prototype device's architecture. Section 5 describes the experimental procedures for testing our prototype, and section 6 discusses the results.

2. Background and Relevant Works

2.1. EEG

EEG is a non-invasive method that detects voltage fluctuations from neuronal activity using scalp electrodes. Its advantages include a high temporal resolution – the ability to monitor brain activity to the millisecond – and a broad signal range (0.1Hz-100Hz) [39]. EEG can be used to detect five different brain frequencies [67], detailed in Table 1.

Table 1: Description of frequency features [22]

Feature	Freq (Hz)	Distribution	Conditions
Delta	0 - 4	Frontal lobe (adults) Posterior region (children)	Deep, non-REM sleep. Not significant in awake teenagers and adults.
Theta	4 - 8	Thalamic regionz	Light sleep, drowsiness, relaxation, and meditation.
Alpha	8 - 13	Occipital (eyes closed)	Relaxed state with some mental processing (i.e. memory, visual processing)
Beta	13 - 30	Symmetrical Extends from frontal to parietal lobe	Excited, alert, or attentive states.
Gamma	8 - 13	Somato-sensory cortex	High-level brain activity (i.e. information analysis and perception.)

2.1.1 Montages

The arrangement of channels, known as *montages*, is essential to localizing these activities within brain regions. The human brain consists of a left and right hemisphere, partitioned into four lobes: Frontal, Temporal, Parietal, and Occipital (see Figure 1). The frontal lobe, located behind the forehead, is involved in motor control, working memory, abstract reasoning, decision making, emotional regulation. Situated behind is the frontal lobe, which processes sensory input (i.e. visual, auditory) into long-term memory. To the top is the parietal lobe, which integrates sensory information from various modalities (i.e. touch, temperature, and spatial awareness). Finally, the occipital lobe, located at the back of the head, processes visual stimuli [69, 25].

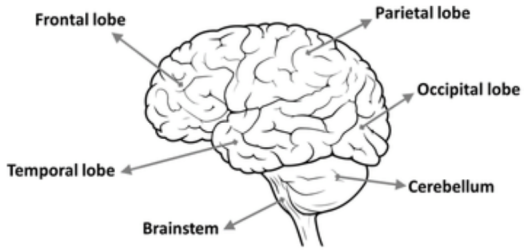

Figure 1: Regions of the human brain

In traditional EEG devices, electrodes are placed equidistant from each other in a standardized 10-20 system (see Figure 2). The system incorporates a total of 16 channels to ensure complete scalp coverage. Electrodes are referred to by the first letter of their assigned region, followed by an odd or even number to indicate their left or right hemisphere position [12]. For example, the encoding "F7" suggests an electrode on the frontal lobe on the left side of the brain. Some encodings end with a "z", indicating a position on the midline of the head. Additionally, EEG devices can incorporate a "common" reference (typically Cz) as a way of normalizing electric potentials. This is commonly selected as Cz, A1, or A2.

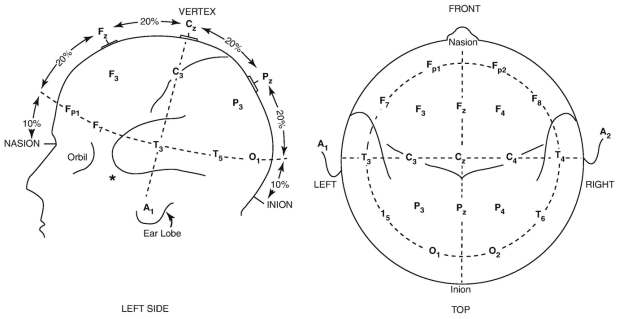

Figure 2: 10-20 EEG placement from the left and top sides of the head. The frontal lobe is monitored by electrodes Fp1 and Fp2 on the forehead, followed by F7, F3, Fz, F4, and F8 from left to right. M1, T3, C3, Cz, C4, T4, and M2 oversee the midsection of the head, while T5, P3, Pz, P4, T6, O1 and O2 cover the posterior side. [2]

Most montages are either bipolar or referential, referring to whether the potential difference at each electrode is measured between electrode pairs or with respect to a reference [68]. In bipolar montages, electrode pairings occur in the longitudinal or transverse directions (see Figure 3(A) and (B)). The longitudinal bipolar montage features two electrode sequences connecting Fp1/Fp2 to the next posteriorly located electrode. Similarly, the transverse bipolar montage connects electrodes from left to right (see Appendix I for a list of common linkages). In both cases, electrodes alternate between being active and reference. Bipolar montages have the advantage of localizing cerebral potential from the direction of deflection of two channels' waveforms, known as phase reversal [68, 12]. However, they may exhibit only half the phase reversals due to a lack of comparative electrodes at the beginning and end of a sequence.

In contrast, referential montages measure potential differences with respect to a "common" reference (CR). Since there are no phase reversals, the waveform's amplitude determines the presence of regional activity. However, the epileptiform discharges may not be as prominent as bipolar montages [12].

Other notable montages include the Laplacian montage, which utilizes the weighted average of neighboring electrodes, and the common average montage, which sums up the potential at each electrode divided by a calculated value (i.e. global average, number of electrodes) [68]. A list of common montage placements can be found here.[1]

[1]Standard montages from the *American Clinical Neurophysiology Society* (ACNS): `https://www.acns.org/UserFiles/file/EEGGuideline3Montage.pdf`

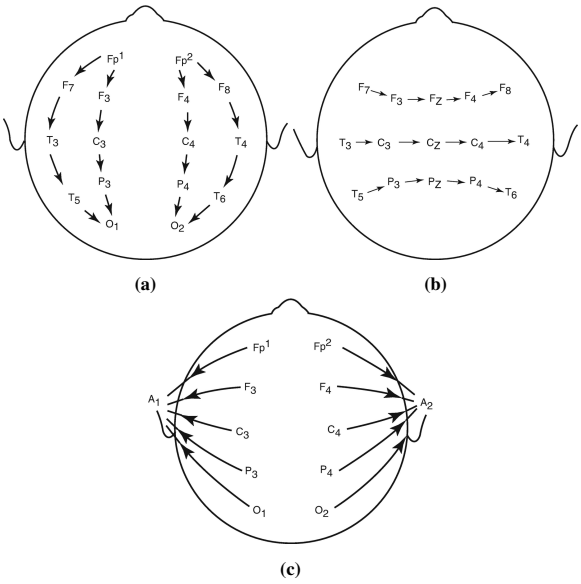

Figure 3: Visual representation of the longitudinal bipolar (a), transverse bipolar (b), and referential (c) EEG montages.

2.1.2 Device Hardware

A standard EEG device consists of electrodes, amplifiers, and Analog-to-Digital converters (ADC) [39]. These components are often attached to a headset or cap, shown in Figure 4:

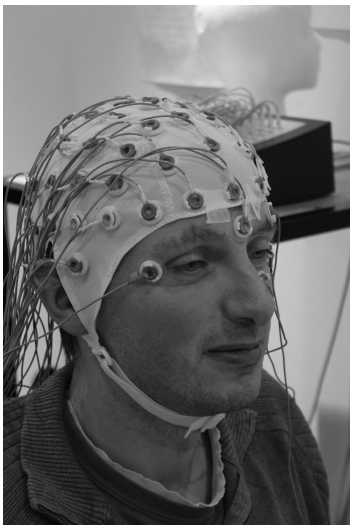

Figure 4: EEG cap with gel-based (wet) electrodes [56]

In the case of wearable EEG systems, the electronics must be small enough to fit inside a handheld case without exceeding low power constraints. They must also be compatible with a wireless transmitter, as the high input impedance of EEG amplifiers is susceptible to wire movements. With new advances in System-on-a-Chip (SoC) technologies, modern EEG systems can fulfill the above conditions at affordable prices. Ahn et al. [4], for example, developed a coin-sized, low-power EEG device using commercially available components. Their circuit, printed on a PCB, utilizes a 24-bit ADC with a sampling rate of 250 sample/s and a Bluetooth module for data transmission. It can monitor a single EEG channel using one active, ground, and reference electrode, respectively.

For optimal EEG recordings, devices must ensure complete contact between the scalp and its electrodes. Currently, wet electrodes are the gold standard for clinical recordings due to their low impedance levels [16]. However, they require the application of a conductive gel or a saline patch beforehand, leading to long set-up times or skin abrasions. Dry electrodes, in contrast, are not affected by these limitations. One example is a pronged electrode (see Figure 5), designed to push away hair from the scalp. Due to its smaller contact area, it is more susceptible to artefacts and high impedance levels than wet electrodes. Despite this, many studies examining both electrode types have obtained comparable results between the two [27]

Figure 5: Dry electrode with prongs for seperating hair. Taken from the DSI-24 [1]

More recently, capacitive or 'non-contact' electrodes have been gaining traction for their ability to amplify signals via AC coupling. In 2010, Chi et al [19]. developed a coin-sized EEG electrode placed directly on skin or through clothing. The device was later improved upon by Sullivan et al [58] (see Figure 6). in 2019 to encompass EEG and ECG. The multimodality and discreteness of their device's design serve as inspirations for this study.

Figure 6: Capacitive electrode for EEG-ECG sensing proposed by Sullivan et. al [58]

2.2. fNIRS

Functional near-infrared spectroscopy (fNIRS) non-invasively maps hemodynamic responses in the brain. It uses NIR spectrum light (600-900nm) to penetrate superficial layers of the head and brain tissues [54]. This light is also readily absorbed by oxygenated and deoxygenated haemoglobin (HbO2/HbO and Hb/HbR). Figure 7 shows the absorption coefficients of HbO2 and Hb, which are similar at 800 nm, indicating the need for multiple wavelengths for accurate detection. fNIRS devices are composed of two parts: NIR sources and photodetectors [3]. These are attached to the scalp in a predefined arrangement, with each source-detector pair (also known as an *optode*) corresponding to a single fNIRS channel. Light emitted from the source is propagated through tissue and absorbed by HbO2 and Hb blood. Due to the scattering properties of biological tissue, the light reaches the detectors through multiple scatterings. Consequently, the optical path length is greater than the actual source-detector separation.

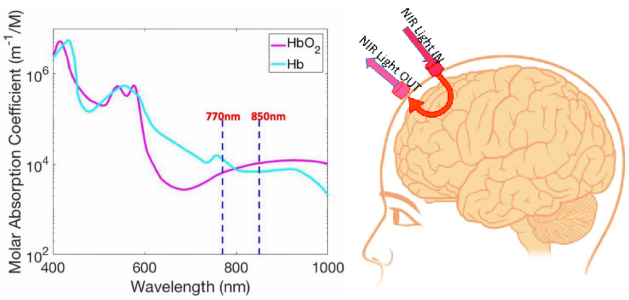

Figure 7: (a) Absorption spectra of HbO2 and Hb, (b) Path of light propagation through the brain.

2.2.1 Placement

fNIRS optode placements often follow the international 10-20 system or the more dense 10-10 or 10-5 systems (see Figure 8). While both the 10-10 and 10-5 systems are derivatives of the 10-20 system, their difference lies in their electrode densities. The 10-10 system places electrodes at 10% increments along the medial-lateral contours of the brain, whereas the 5-5 system uses 5% increments (see Figure 6). These changes allow 10-10 systems to have approximately 80 standard positions and 5-5 systems to have over 300 [33].

fNIRS systems are also highly dependent on source-detector separations. As separation distance increases, light propagation increases, resulting in a higher attenuation in the reflected light due to scattering. Studies have found a source-detector distance of 3 - 5cm to be suitable for neuroimaging [3, 62]. However, this can vary depending on the hardware setup and the desired data. One example is a

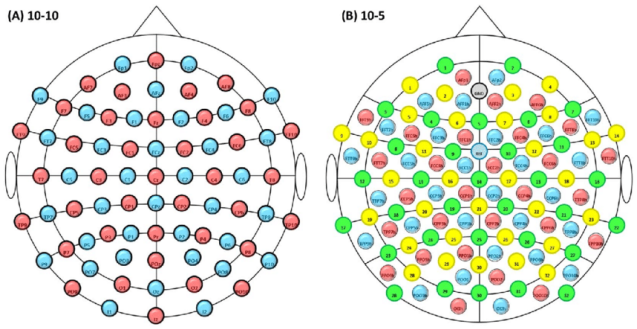

Figure 8: The 10-10 (left) and 10-5 international systems. EEG positions are depicted in green, whereas fNIRS sources and detectors are depicted in red and blue respectively [71].

"short channel", or a source-detector pair with a distance of 5mm-10mm [18]. This kind of placement is helpful for artefact removal as it can detect minor motion artefacts outside the brain.

2.2.2 Device hardware

fNIRS source optodes typically consist of one multi-wavelength LED or several single-wavelength LEDs. Their peak wavelengths range from 700 to 850nm, corresponding to the intersection between the absorption spectra of Hb and HbO2 (see Figure 7). The LED/LEDs alternate between intensities on a schedule enforced by a central processing unit (i.e. a microcontroller). This schedule extends to fNIRS detectors and how the system processes incoming signals.

Due to the availability of low-cost optical sensors on the market, various wearable fNIRS systems have emerged for research and consumer use [3, 54, 64]. These devices have been experimented with across various unconstrained environments, including social interactions [49] and exercise [50]. In addition, they have been made patchable or compatible with a headband [3, 54].

2.3. EEG-fNIRS

While EEG and fNIRS BCI systems are capable on their own, their performance remains susceptible to inter-subject variation or artefacts. For more effective brain readings, studies have introduced *multimodal* imaging, combining two or more signals, to assess both the electrical and hemodynamic functions of the brain. In particular, EEG-fMRI has successfully provided more robust features for analysis [52, 7, 46, 30]. However, limitations to this technology (i.e. high cost, fixed location) have barred it from consumer use. As such, studies have increasingly turned to EEG-fNIRS as an alternative for long-term monitoring.

The idea of EEG-fNIRS comes from the selective view of brain functioning the two modalities provide separately [30]. EEG has an extraordinary temporal resolution but a

Table 2: Distinguishing characteristics of previous literature, compiled by Ahn et al [6] (ERP, event-related potential; SSVEP, steady-state visual evoked potential).

Reference	Regions of recording	Task	Feature	Findings
Khan et al. 2014 [36]	EEG: sensorimotor; fNIRS: prefrontal	Mental arithmetic and motor imagery	EEG: peak amplitudes; fNIRS: HbO and HbR	Classification accuracies over 80% were obtained from decoded EEG and fNIRS signals from tasks involving mental arithmetic and hand tapping.
Tomita et al. 2014 [61]	Occipital	Visual attention to flickering checkerboard stimulus	EEG:SSVEP fNIRS: HbO and HbR	Classification accuracies of SSVEP was improved when fNIRS was used to active the SSVEP BCI.
Morioka et al. 2014 [46]	EEG: whole scalp fNIRS: parietal and occipital	Spatial attention	EEG: alpha/beta fNIRS: HbO	EEG-fNIRS decoder with cortical current estimation performed better than EEG decoders.
Putze et al., 2014 [52]	EEG: whole scalp fNIRS: temporal and occipital	Visual and auditory perception with movies and audiobooks	EEG: ERP fNIRS: HbO and HbR	The subject-dependent approach achieved a higher classification accuracy (over 90%) in discriminating bteween states.
Koo et al., 2015 [37]	Sensorimotor	Motor imagery	EEG: alpha fNIRS: HbO	The study designed an fNIRS sensor frame to block leaking light. EEG-fNIRS was used to develop an online self-paced motor imagery BCI with fNIRS as a brain switch. The system achieved an overall accuracy was 90%.
Ahn et al. 2016 [7]	EEG: whole scalp fNIRS: prefrontal	Simulated driving	EEG: alpha/beta fNIRS: HbO	Normalized EEG and fNIRS were used for drowsiness detection using a series of combined classifiers. Combined EEG-fNIRS achieved a greater classification accuracy EEG and fNIRS alone.
Nguyen et al. 2017 [48]	EEG: whoel scalp fNIRS: prefrontal	Simulated driving	EEG: beta fNIRS: HbO	Beta-band power and HbO in the frontal region detected drowsiness more rapidly than eye-blinking.

low spatial resolution and signal-to-noise ratio due to the conductivity of the skull [6]. In contrast, fNIRS has a high spatial resolution but a low temporal resolution. Due to their complementary natures, simultaneous EEG-fNIRS could overcome the weaknesses of the individual modalities to provide more robust data. Table 2 presents a summary of findings from previous EEG-fNIRS studies compiled by Ahn and Jun [6].

Although EEG-fNIRS systems generally have low-design costs, their effectiveness remains dependent on three factors: (a) the placement of the electrodes and optodes, (b) the synchronization of fNIRS and EEG recordings, (c) and the reduction of crosstalk between systems [65]. These challenges are detailed below.

(a) Similar to wearable EEG devices, wearable EEG-fNIRS systems must balance wearability with sufficient scalp coverage. They must also consider the sensors' characteristics, such as the electrode type (wet or dry) for EEG systems. Despite recent developments in optode and electrode technology, they can take up a large amount of space, preventing EEG and fNIRS sensors from being positioned at appropriate 10-20 points.

(b) A significant limitation of fNIRS BCI is its hemodynamic response delay ($\approx$7s) compared to near-instant EEG recordings. One solution is to use a slope indicator feature, proposed Buccino et al. [14], representing the difference between the current time segment average and the previous one. However, implementing this on a smaller scale remains a challenge for wearable devices.

(c) Since fNIRS systems involve the use of time/frequency multiplexing or modulation, it creates the possibility

of crosstalk between EEG and fNIRS systems. Luhmann et al. [66] reported that this crosstalk is outside the frequency range of interest of EEG systems and is removable with low-pass filters. However, time-multiplexed fNIRS systems can exhibit source switching within this region, thereby posing constraints on analysis [65].

We employ a pre-existing fNIRS and EEG sensor with synchronization performed via software in this study. However, future designs must carefully consider the above factors to achieve complete wearability.

3. Market Research

3.1. Available devices on the market

To obtain a holistic and comparable view of consumer neuroimaging technologies on the market, market research was conducted for modern BCI products aimed for both retail and research/medical consumers. These devices are evaluated in terms of comfort, appearance, modality, sensor count, applications, battery, data resolution, and data storage. This section reviews the Muse, Emotiv Insight, and Flow headsets, the AttentivU glasses, the Neurable and Sens.ai headphones, and the Humm patch (see Figure 9 for the form factors of each device).

3.1.1 Muse Headset

The Muse headset (InteraXon, Inc., Toronto, Canada) is a comfortable and portable EEG headset that features a thin band around the forehead that connects to wide hooks that make contact behind the ear. Although there is no official maximum comfort time, one customer stated in a review that they achieved around "40 hours of use over a month" out of the Muse headset. Using this estimated time, the maximum comfort time is assumed to be about two hours. The Muse headset incorporates six EEG sensors on the prefrontal cortex, and it aims to make meditation practices and sleep habits easier through real-time neurofeedback. While the device allows for data to be collected at a rate of 256 samples per second, neural features are produced at a rate of approximately 10 Hz due to the speed of data processing. The device has a battery capable of sustaining 5 hours of continuous use and transmits data to external devices via Bluetooth.

3.1.2 AttentivU Glasses

The AttentivU glasses (MIT Media Lab, Cambridge, USA) are a subtle and portable EEG/EOG device that is meant to appear as a normal pair of glasses. The glasses have a stockier build and require a thicker frame to house the two EEG and two EOG sensors that allow for the measuring of eye movement, cognitive load, fatigue, focus, and other cognitive processes. The sensors are aligned on the motor cortex and somatosensory cortex in both hemispheres. The AttentivU glasses are one of the few devices found that use a multi-modal configuration, measuring both EEG and EOG data. The 3.7V 150mAh Lithium Polymer battery supports continuous use for 5 hours. Optionally, there is an external battery that can be attached to the device and provides 15 hours of battery life. No data could be found about the sampling rate but the device connects and transmits data via Bluetooth.

3.1.3 Emotiv Insight Headset

The Emotiv Insight headset (Emotiv Inc., San Francisco, USA) has a unique non-conventional headband design that is sure to turn heads. The headset has two prong-like electrodes that extend over the forehead to measure the prefrontal cortex. Additionally, there are three other electrodes that extend behind the back of the head and measure data from parts of the motor cortex and somatosensory cortex. The Emotiv headset has three 'gummy' prong EEG sensors that make for better hair penetration and thus a stronger connection. No data could be found concerning the comfort level besides a claim from the source company that the headset was indeed very comfortable. The headset has been used for research purposes and for personal uses such as meditation and focus improvement. The headset sports a battery life of four hours in low power mode but that time can be extended using a wireless Bluetooth receiver. The headset connects to external devices via Bluetooth and transmits data at a resolution of 128 samples per second.

3.1.4 Neurable Headphones

The Neurable headphones (Neurable, Inc., Boston, USA) are a pair of fully functional headphones with eight EEG electrodes in each earmuff and can be worn comfortably for approximately 39 minutes. The device reads and interprets neuronal activity in the auditory cortex, auditory association area, sensory association area, primary somatosensory cortex, and primary motor cortex in both hemispheres to generate a focus score at all times during use. The intent of this product is to provide neurofeedback for focus so the user may track and improve their habits throughout the day. Neurable guarantees this device has "all-day battery life and rapid charge" capabilities and records data at a rate of 500 Hz. Data is transferred wirelessly to Bluetooth connected devices.

3.1.5 Humm Patch

The Humm patch is a flexible, lightweight patch based device which performs neural stimulation called transcranial

Figure 9: Device appearance for (a) Muse Headset, (b) AttentivU Glasses, (c) Emotiv Insight Headset, (d) Neurable Headphones, (e) Humm Patch, (f) Flow Headset, (g) Sens.ai Headphones, and (h) Neurosky MindWave Mobile 2

alternating current stimluation (TACS). The patch must be placed on the forehead and thus recordings and stimulations are limited to the frontal cortex. Humm also claims to improve mental performance and extend working memory. The device runs on disposable batteries. This product is aimed for retail consumers and not researchers, since they advertise consumer benefits of using the product and focus more on stimulation than data collection.

3.1.6 Flow Headset

The Flow Headset (Flow Neuroscience, Malmö, Sweden) is another forehead-based BCI headware. The device is an unobtrusive headset which applies electrical stimulation to the forehead. The battery lasts approximately 5 hours, there are 2 sensors, and the data is transmitted to the user for local storage via a bluetooth connection. Flow is an implementation of transcranial Direct Stimulation (tDCS), a treatment for depression based on low power electrical stimulation on areas of the head. It targets the frontal and prefrontal cortex based on its position on the forehead. It is targeted at retail consumers.

3.1.7 Sens.ai Headphones

The Sens.ai headphones (Sens.ai, Inc., British Columbia, Canada) are a comfortable EEG-enabled set of over-ear headphones. The device contains 3 EEG sensors over the frontal cortex and the occipital lobe. The headphones also come with 7 PhotoBiomoduleation LEDs which Sens.ai claims can force mindstates by stimulating the wearer based on EEG data. The built-in EEG sensor has a very high data resolution, and can record at 1024 Hz for 8+ hours with a lithium ion battery. Data is stored in a companion mobile app. The sens.ai headphones are another retail product aimed at consumers rather than researchers.

3.1.8 NeuroSky MindWave Mobile 2

The NeuroSky MindWave Mobile 2 (Neurosky, Inc., San Jose, USA) is a portable DSI headset with one EEG electrode in the FP1 position. The device is research oriented, with the goal of being an easy, consumer grade headset to measure, track, and improve attention. The EEG sampling rate is 512 Hz, and the headset can stay on for 8 hours. The Mobile 2 uses data from its EEG sensor to shed insight on meditation, focus, and eye blinking for the wearer.

3.2. Important features

In this section, multiple design metrics are identified and evaluated. The interpretation of each design metric and its relative importance are discussed. The goal of this section is to highlight what design metrics are considered valuable for a neuroimaging device to be successful in market.

- **Comfortability**

  One of the most important features to incorporate a ubiquitous headset into the modern workplace is comfortability. The headset should be able to withstand the movements required to do everyday activities for extended periods while not causing any sort of discomfort to the user. In the context of this project, this is interpreted as 12-16 hours of continuous use. To maximize comfort, a design with as few wires as possible should be implemented. While fewer wires are better, the headset should still be adjustable to make room for

extra wires if needed. Additionally, padding in crucial areas that are important to comfortability should be incorporated. This means extra fabric capable of providing padding around sensors and other internal components that could prove to be a source of uncomfortability. While comfort is key, convenience is also a factor of great importance. The average person should be able to easily follow along with the instructions on how to put on the headset. Ideally, the ubiquitous headset should have a quick and easy configuration. No help should be required to put on the headset even for those of younger or elderly ages.

- **Durability**

  Another important metric to consider is durability. The device should be inexpensive to the point that it is a prime candidate to consumers over other products from a price-oriented perspective, but it should be fabricated at a quality level that ensures durability through constant use for over a year. The device should also be able to withstand some blunt force trauma to a certain extent. This will require protective casings around sensors and incorporated bluetooth devices that will minimize sustained damage.

- **Flexibility**

  The device must be flexible in both the sense that it can conform to the shape of the head of any user and also the sense that electrode placement on the head is easily able to vary to encompass a number of different applications. Different applications may require sensors to get data from separate regions of the brain, so this flexibility is a crucial feature in design.

- **Low-Power** The device must have all-day-use capabilities. Low power consumption is a design priority so as to minimize the battery size required for usage up to 16 hours.

- **Signal Quality** High quality of data is another priority in the design of this device. The multimodal approach utilizes two sensors in total (EEG, fNIRS), and their placement must be carefully considered.

The EEG-fNIRS device is envisioned to be attached to the user via a disposable bandage. The purpose of the disposable bandage is to improve the cost efficiency of the device, increasing its appeal for both clinical and commercial applications. Additionally, the bandage must allow for minimum sensor movement and impedance, and be skin-compliant. This will ensure that the data collected is consistently of high quality.

3.3. Application Areas

Modern EEG and fNIRS wearable devices vary in terms of their functionality and intended use cases. Broadly, the devices can be broken into two categories: those intended for retail consumers, and those for research. The retail products generally incorporate some kind of neurofeedback system in order to create value for the consumer – see: Sens.AI, Emotiv Insight, etc. The research products do not need to create immediate value for the consumer because of their use case, so they tend to focus on collecting higher quality data. The sections below detail areas that an EEG-fNIRS device would be applicable to.

3.3.1 Neurofeedback

Neurofeedback is a form of brain therapy in which a subject learns how to perform tasks more efficiently by being consistently reinforced with real time feedback from their brain activity.[10] This is one of the most common use-cases for EEG, and most existing products on the market can be used for neurofeedback. The goal of neurofeedback is to teach patients to produce brain-wave patterns linked with the qualities needed to perform a given task. [57]

3.3.2 Alzheimer's

The cause of Alzheimer's disease is due to the increased pile up of amyloid beta peptide between the presynaptic axon terminal and the postsynaptic dendrite. It takes roughly 15-20 years of this amyloid beta to build up until it nears significant levels of accumulation, at which time the symptoms of Alzheimer's disease begin to occur. [26] A couple of negative health patterns that can increase the chance of being diagnosed with Alzheimer's disease are sleep deprivation, high cholesterol, high blood pressure, unhealthy diet, lack of physical exercise, smoking, and excessive alcohol consumption. However, there has been a substantial increase in neurofeedback research to treat Alzheimer's disease.[28] An essential concept for a solution is attempting to increase neuroplasticity to reduce or even prevent Alzheimer's disease. Some activities that can increase neuroplasticity are mental math games, language comprehension tasks, tests of memory, solving puzzles, physical exercise, etc.. Neurofeedback training can also refresh and revitalize parts of the brain to increase neuroplasticity through clinical check-ups and modifications of treatments by doctors and physicians. A wearable BCI device that can be worn outside of a lab environment would be a great tool for neurofeedback research in Alzheimer's patients. Although promising, there exists severe limitations to BCI research and treatment of Alzheimer's due to the nature of patients inability to self regulate brain activity. Currently, research is being conducted into whether a device could differentiate 'yes', 'no'

and other emotional responses by correlating or mapping them to positive and negative stimuli.[43]

3.3.3 Schizophrenia

Currently, an obstacle in treating schizophrenia is that patients often do not regularly take medication. Neurofeedback can provide a new and effective method where the patient and their family do not have to take any specific action to supervise their own neurofeedback training. BCI has been able to detect certain network behaviors specific to patients diagnosed with schizophrenia in various studies, acting as a key and efficient way to diagnose patients.[59] Patients with schizophrenia have been seen to have decreased levels of alpha activity as well as or exclusively increased beta and delta activity in their EEG recordings. Through neurofeedback, clinicians are able to make more informed decisions on how best to proceed with the treatment of a patient so that the appropriate brain regions and neuronal networks are affected.[9] Neurofeedback may also be utilized to assess the reaction of a patient to specific medications that are part of their regular treatment.[45]

3.3.4 Sleep

A major rising issue for the general population is chronic insomnia, which may be caused by a problem with the brain being unable to shut off its wake cycle and transition into sleep.[21] EEG devices are often used in sleep studies to track and analyze certain patterns of brain activity while a person is going through different stages of sleep. Trained neurologists use the EEG sleep data from these devices to identify and characterize abnormal patterns of activity that occur during restfulness. Damaged areas of the brain that may cause seizures may be identified through detection of abnormalities in EEG data.[20] Benefits of sleep EEG recordings include long recording periods and a more complete evaluation of the brain. Additionally, it also provides data to physicians for analysis for better treatments for insomnia or other sleep related issues. Neurofeedback treatments may lead to increases in total sleep time and increased REM sleep. [31]

3.3.5 Pz area of Brain

The Pz area of the brain consists of two parts. The first is the anterior parietal lobe. It is responsible for most of the basic movements and senses that humans have, such as sensation of touch, spatial awareness, hand-eye coordination, visual perception, speech, reading, writing, and math. The other part of the Pz area of the brain is the occipital lobe. Its job is to process visual information, as it contains both the primary and association visual cortices. Various studies have shown that an increase in alpha activity in the occipital lobe is linked to improved anxiety symptoms due to the increase in neural activity stimulating relaxation [32].

3.3.6 Focus Level

While the use of electronics and different media outlets constantly decrease the attention span and focus levels of typically younger generations, neurofeedback can provide an applicable solution. The brain produces beta and gamma waves when focusing and sustaining attention.[24] Thus, by analyzing the brain waves of someone with ADHD, neurofeedback could help a patient improve their focus habits. This practice may also be generalized to the public. [44]

3.3.7 Stress

Many people with anxiety and stress will produce more beta waves, which may contribute to fear and panic depending on which brain regions are expressing this activity.[70] Neurofeedback can help reduce these thoughts by making the user aware of their negative emotions when they first occur and pulling them out of these harmful thought patterns. It can also provide physicians and doctors with specific details and information that can be used to alter treatments for high stress and high anxiety. [35]

3.3.8 Social Interaction

Neurofeedback could also be used to provide real-time feedback on the emotional states of others to allow for a more intimate or more intellectual conversational experience. Examples include getting feedback when participants in conversation become sad or nervous around specific topics, and when statements are well-received or cause elation.[38] It can help draw a line so people know which topics and subjects their conversational partners prefer or dislike in their social interactions with others. This way, unpleasant conversational experiences may be more easily avoided so as to allow for more positive and smarter exchanges.

3.3.9 Real-Time Commands

Neural activity may also be used to generate various commands at certain levels of complexity depending on device limitations. Disabled persons could make use of an EEG wearable device to interface with a computer and make their life easier for daily tasks and communication. Applications include but are not limited to two-dimensional cursor control, navigation functions within a user interface, and the control of neuroprosthetic devices.[11]

3.3.10 Epilepsy

Epilepsy is categorized as a central nervous system disorder that causes mild to severe symptoms such as seizures, loss of awareness, and unusual behavior. [60] Since epilepsy can affect any area of the brain, there are many potential side effects of the disorder. Diagnosing epilepsy early is very important as the symptoms can be life threatening. Neurologists have been successfully using EEG to diagnose and assess epilepsy ever since the discovery of the technology in 1929 [53]. Neurologists look for abnormal brain activity or epileptic waves, characterized by a particular pattern of sharp spiking activity known as interictal epileptiform discharge (IED) to classify and diagnose epilepsy.[8] Neurofeedback is integral in determining the proper medication and treatment for patients suffering from epilepsy.

3.4. Value Analysis of Device Characteristics

A value analysis table outlines the positive and negative aspects of similar products in a standardized, easy to read way. Table 3 provides a basic but informative value analysis of all the previously mentioned products, judging them on their modality, invasiveness, comfort, neural signal, and usability to determine overall rankings. Each category is unweighted, and each device's total score is simply the sum of its scores for each individual category.

4. System Architecture

This section outlines a potential design for a wearable BCI device which uses the BioSignalsPlux EEG and fNIRS sensors. The general system overview (i.e., the interactions between each component) is discussed first, followed by more detailed looks into each individual component, and finally a 3D model of the device.

4.1. System Overview

For the purpose of this investigation, the wireless EEG and fNIRS sensors from biosignalsplux (PLUX, Rua Corredouras, 2630 Arruda dos Vinhos, Portugal) were selected for testing. The wireless functionality is presented in Figure 4. Each component is explained in further detail in the sections below.

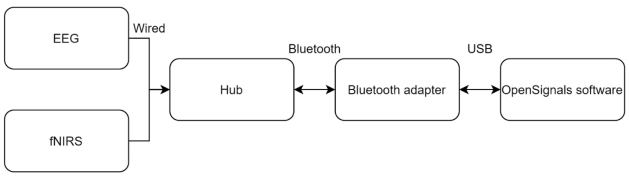

Figure 10: Block diagram of the biosignalsplux wireless application

4.1.1 BioSignalsPlux Hub

The biosignalplux hub features 4 analog channels that support 16-bit resolution and 3000Hz sampling frequency and accepts a variety of sensors (EEG, fNIRS, accelerometer, triggers, etc). The hub uses onboard bluetooth or an optional high speed dongle to connect and stream data to devices running the OpenSignals software. We experience initial struggles connecting the hub with the onboard bluetooth but had success via the bluetooth dongle. The bluetooth range is roughly 10m or line of sight. The hub has a battery life of roughly 12 hours with a 2.5 hour charging time.

4.1.2 EEG Sensor

The kit contains a single EEG sensor that connects to the biosignalplux hub via any analog channel 1 through 4. The sensor features a bipolar configuration with the 2 short electrodes (Red and Black) measuring electrical potentials in a given region with respect to the single long white banded lead as the reference electrode. The reference electrode must be connected to a region with very low muscular activity such as the bone behind one's ear. The leads must be fitted with a single-use sticky electrode pad that attaches to the subject. Upon initial testing we were successfully able to receive a quality signal from the EEG in OpenSignals.

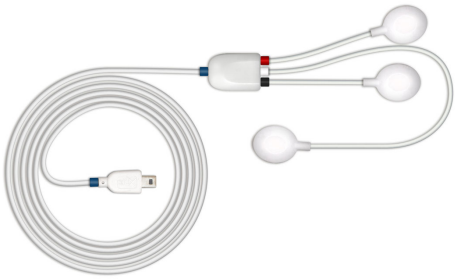

Figure 11: The Plux EEG sensor

4.1.3 fNIRS

The kit contains a fNIRS transmitter that connects to the ground port. The fNIRS transmitter and receiver must be placed on the forehead. A fNIRS sensor uses a coupled set of two emitters (1 Red and 1 Infrared LED) and one photoreceptor in a reflectance mode. Sensor digital output is composed of two channels. For now the sensors are held in place with the black elastic band. There is one physical difference between the stock Plux fNIRS sensor and the one used in the prototype which does not affect functionality. The transmitter and receiver are separated and not in the same case.

	Modality	Invasiveness	Comfort	Neural Signal	Usability	Total Score
Emotiv Insight	1	4	5	3	5	18
Neurable Headphones	1	2	8	4	5	20
Neural Interface In-Ear	1	6	2	6	6	19
Humm Patch	1	1	9	5	5	21
Flow Headset	1	2	6	2	2	23
Sens.ai Headphones	1	2	6	2	4	15
NeuroSky MindWave Mobile 2	1	3	5	1	1	13

Table 3: Value analysis of wearable EEG/fNIRS devices

Figure 12: The stock Plux fNIRS sensor

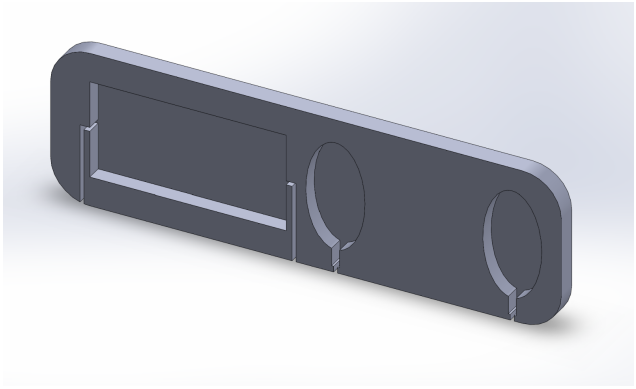

Figure 13: CAD model of potential patch design

4.1.4 OpenSignals Software

OpenSignals is a software for interfacing with the Plux hub and any of its connected sensors. It can run on windows, mac, or linux. At the moment, we are running opensignals on one of the laboratory desktop computers. In the future, opensignals could run on a dedicated device. OpenSignals also gives the option to stream data live over TCP/IP. This is another option that could be explored in the future.

4.2. Patch Design

This study proposes a lightweight, adhesive patch-based device which supports the Plux EEG and fNIRS sensors. To be as small and unintrusive as possible, the patch is built around the sensors with as little extra material as possible. The patch's total form factor is 135mm x 40 mm x 5mm. The patch has three main impressions: one for the fNIRS transmitter and receiver, and two for the EEG electrodes. The impressions also allow for wires to be drawn out from the sensors to the BioPluxHub, which will be in a secure location on the user's body such as their pocket. This allows the patch to only contain sensors, keeping it as sleek and lightweight as possible. A 3D render of the patch is shown below:

5. Experimental Studies

The viability of the Plux EEG and fNIRS device was tested with three experiments: Eyes Open Eyes Closed (EOEC), Sustained Attention to Response Task (SART), and Mind Wandering (MW). Our code implementations can be publicly accessed using the following link: `https://github.com/Ubiquitous-EEG-IQP`.

EOEC is a standard procedure for EEG devices which tracks neural activity when the subject has their eyes open, and then closed. With an accurate EEG device, there should be clear activity in the alpha waves (8-12Hz range) when the subject has their eyes closed, and this is generally a determinant of sensor efficacy. The SART and MW experiments are VR simulations aimed at tracking user attention, which was identified as a key usage of multimodal wearable sensors. The SART experiment keeps the user constantly engaged by having them click a trigger in response to a rapidly changing digit. MW tracks user focus while reading an essay which contains misspelled or gibberish words. The user is tasked with identifying these words, and lapses in identification – i.e., type II errors, which are discussed later – are indicative of mind wandering. All three of these ex-

periments were performed multiple times, and the data and derived results are discussed below.

5.1. Hardware Setup

All three experiments made use of the Plux EEG and fNIRS sensors, but the SART and MW experiments also made use of commercially available VR headsets. The Plux sensors are discussed first due to their commonality, followed by the VR headset and a note on eye tracking (which is a VR feature used in the MW experiment but not SART).

5.1.1 Plux EEG and fNIRS sensors

The technical specifications of the Plux sensors have already been discussed, but not the pragmatic implications of using the sensors in the experiments. The EEG sensor contains 3 electrodes: active, reference, and ground. Each electrode is attached with an adhesive gel pad to the required location. The fNIRS sensor has two components: a transmitter and a receiver. Both elements are held to the subject's head in the appropriate locations (generally right next to each other), and then held in place with an adhesive. To make sure that the sensors do not fall off or lose connection, they are secured with an elastic band around the head which covers the sensors and keeps them in their desired location.

5.1.2 VR Headset

The SART and MW experiments make use of virtual reality environments to immerse the subject in a completely sandboxed environment. We used an HTC Vive Pro. In order to get accurate sensor placement, the sensors are placed and secured before the subject puts on the VR headset. The SART experiment was developed in Unreal Engine, and the MW experiment was done with Unity. Both are loaded into the headset environment via the SteamVR API, which handles connections between a desktop computer (and its GPU) and the VR headset.

5.1.3 VR Eye Tracking

In addition to the standard VR environment, the MW experiment makes use of the eye tracking functionality of the HTC Pro Eye. Not all VR headsets have eye tracking functionality, and so it is important to make sure that eye tracking is possible before running the MW experiment. If there is no eye tracking functionality on the headset, the Unity software will fall back to a vector orthogonal to the viewport centered on the subject's nose (by estimation). This can create the illusion of eye tracking, but it is not accurate.

5.2. Experimental Protocol

This section describes the protocol for setting up and running the EOEC, SART, and MW experiments with the prototype device.

5.2.1 Eyes Open, Eyes Closed (EOEC)

The first of two experiments performed was an "eyes open, eyes closed" experiment. This entailed the participant sitting with eyes open for one minute, then closing eyes for one minute, opening eyes again for a minute, then closing eyes again for one minute. Multiple sensor placement arrangements were attempted; however, the best results were achieved by placing the EEG electrodes on T4 and F8 (as dictated by the international EEG 10-20 system) with the reference electrode placed on the back of the neck at the base of the skull

5.2.2 Sustained Attention to Response Task (SART)

The second of the two experiments performed was SART (Sustained Attention to Response Task). This is a clinically recognized experimental procedure in which digits 0-9 are presented for 250 ms immediately followed by a circle with an X which is presented for 900 ms. The digits are displayed in the center of the screen sized to one of five random font sizes. The participant is instructed to press a key as quickly as possible if the number is not a 3, and to not press the key at all if the number presented is a 3. Reaction times and the success of each trial is recorded in a spreadsheet for later analysis. The goal of this experiment is to detect neural activity in both the beta and gamma frequency bands, as these are indicative of heightened levels of engagement and focus.

5.2.3 Mind Wandering

Mind wandering is a phenomenon which occurs in humans when they lose focus while completing mental tasks. The mind wandering experiment attempts to track mind wandering events as a subject reads a short essay within a VR environment. The experiment induces and measures mind wandering by having the subject identify misspelled words in a long text. When a subject does not identify a misspelled word, we can say that they are not focused and consider them to be "mind-wandering" at that point in the experiment. The experiment controller uses eye tracking to watch the user's vision, so we can track exactly where they are in the text throughout the experiment

For the subject, the sequence of the experiment is as follows (the subject is wearing a VR headset with eye tracking enabled):

- Read the tutorial. The tutorial explains the experiment and the controls.

- Perform trial run. This is the same as the actual experiment, except it is much shorter and there are no misspelled words. It is just a sandbox for the subject to get used to the reading pace and the controls for marking words as misspelled.
- Read full text. This is where the bulk of the experiment happens. It takes roughly 20 minutes to get through the full text.
- Answer questions. There are a couple multiple choice questions at the end of the experiment for the subject to answer. The responses are recorded in a json file.

A screenshot from the subject's view is included below. In the screenshot, the word "potter" is marked red because the subject identified it as misspelled.

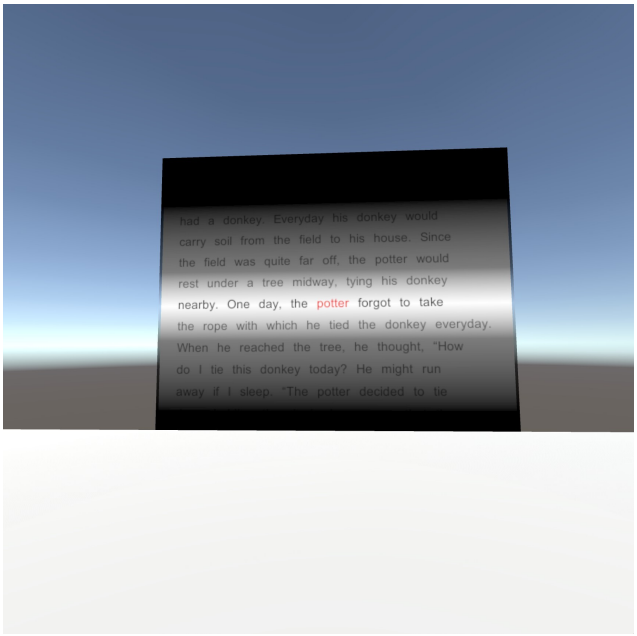

Figure 14: A user's view during the Mind Wandering experiment

5.2.4 Mind Wandering: Type I and II Errors

During the MW experiment, the subject is tasked with identifying misspelled words. As such, the subject takes on the role of a classifier for each word, where the classifications are either misspelled or not misspelled. Thus user errors in identification can be categorized as type I or type II, based on the following null and alternative hypotheses.

$$H_0 \equiv \text{Word is not misspelled}$$
$$H_a \equiv \text{Word is misspelled}$$

The user can make two errors:

- Type I: Marking a correctly spelled word
- Type II: Skipping an incorrectly spelled word

Type II errors signify mind wandering and are thus the primary focus, however type I errors are also discussed.

6. Experimental Results and Discussion

Each experiment was conducted multiple times with varying sensor placements and subjects. The data and analysis of each experiment are discussed below.

6.1. Eyes Open Eyes Closed

Eyes open eyes closed is a standard procedure for testing the output data of an EEG based BCI device. As per its name, the subject spends time with their eyes open and closed while connected to an EEG device. Generally, alpha activity is noticeable when their eyes are closed and undetectable when they are open. The experiment established a baseline for the Plux sensor by ensuring a clear signal quality.

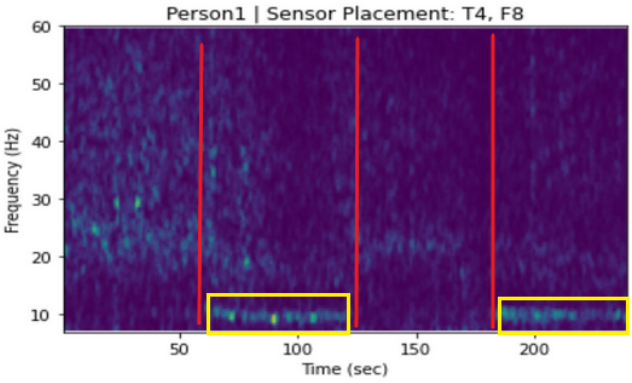

(a) Spectrogram for EOEC experiment with Subject 1

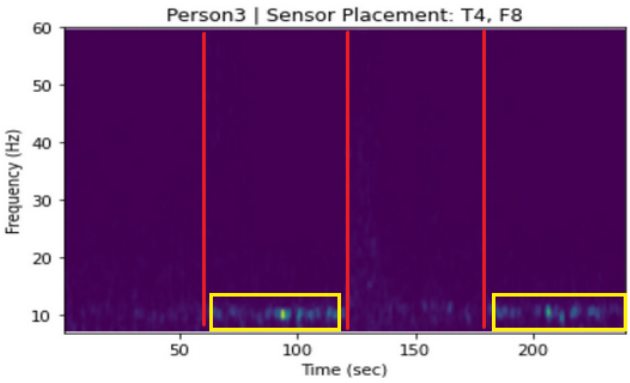

(b) Spectrogram for EOEC experiment with Subject 3

Figure 15: Spectograms from EOEC experiment

The spectrograms drawn from the EOEC data show clear, discernible segments containing either strong alpha activity or almost no alpha activity (Figure 15). The segments of high alpha activity correctly correspond to when

the subject has their eyes closed, and the segments of no alpha activity are when the subject has their eyes opened.

6.2. SART

The sustained attention and response task is a VR based experiment that tracks user attention over time by having the user respond to quickly flashing numbers (0-9). The user is instructed to click their handheld trigger with each digit, except for it is 3.

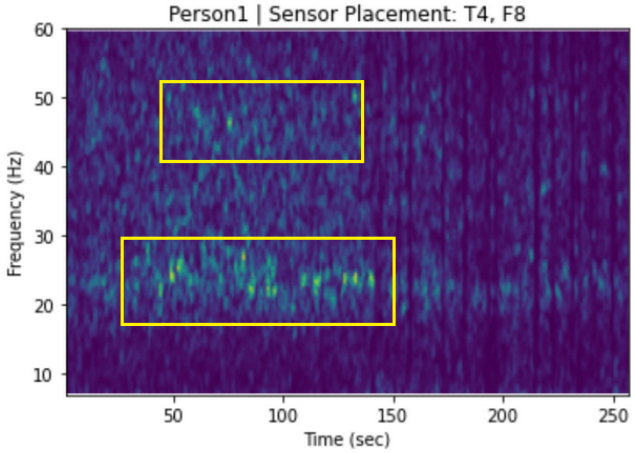

(a) SART EEG spectogram for Subject 1

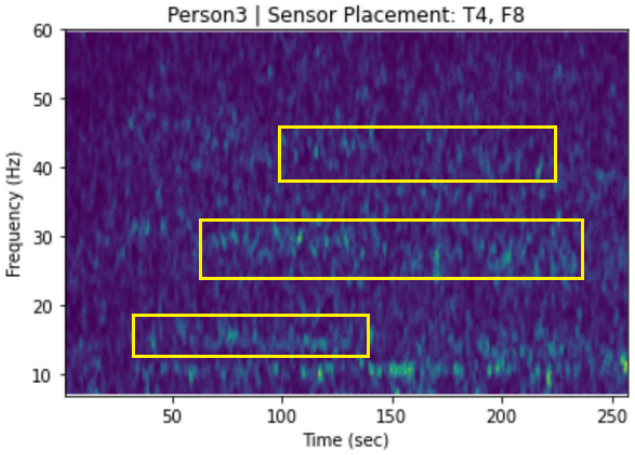

(b) SART EEG spectogram for Subject 3

Figure 16 shows spectrograms that were created from EEG recordings obtained from participants while conducting the SART experiment. Spectrograms illustrate the change in power spectral density at various frequencies over time. The highest levels of brain activity in the areas measured are indicated by yellow while the lowest levels of brain activity are indicated by a dark purple. Levels of brain activity in between the two ends of this spectrum take on either blue or green, depending on if they are lower or higher on the spectrum, respectively. There is a detectable level of

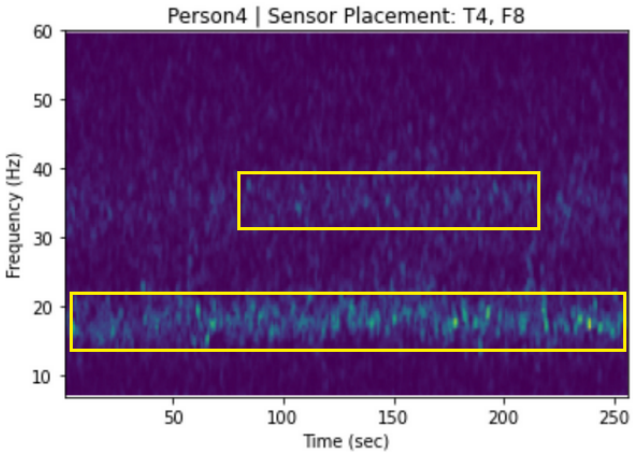

(c) SART EEG spectogram for Subject 4

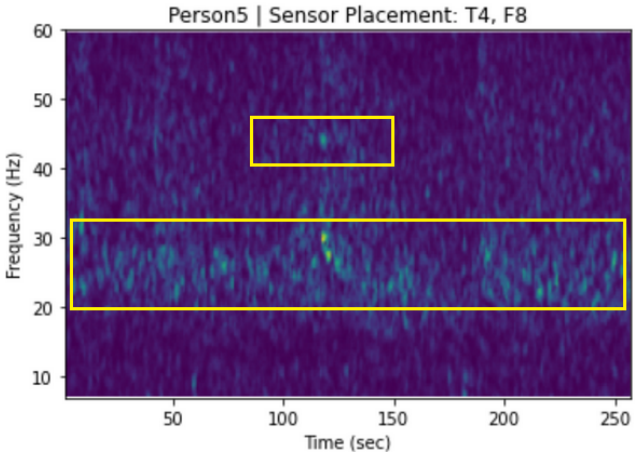

(d) SART EEG spectogram for Subject 5

Figure 16: SART spectogram results for Subject 1, Subject 3, Subject 4, and Subject 5

heightened activity present within the beta band and trace amounts in the gamma band. This is in alignment with the prior knowledge that activity in these frequency bands is indicative of higher levels of engagement.

6.2.1 Performance Data

Figure 17 depicts performance data collected from the participants. The reaction times for Subjects 1 and 4 corresponding to correct answers form a cluster and therefore have a lower variance. In contrast, the reaction times for correct answers in Subjects 3 and 5 are more varied. One reason for these differences could be that Subjects 1 and 4 were, on average, more mentally engaged than Subjects 3 and 5. Another reason could be an inherent difference in the response dynamics of Subjects 1 and 4 than Subjects 3 and 5.

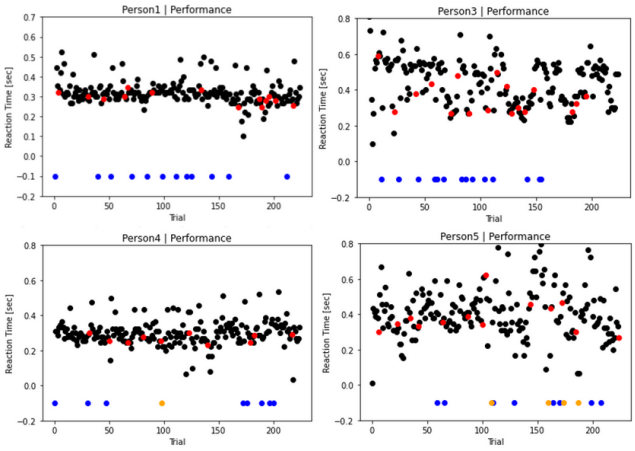

Figure 17: Depicts performance data collected from the participants. Black points refer to correct answers that were not 3's in all of the graphs represented in the figure, as in the participant answered correctly to numbers that were not 3 within the trial window. Blue points refer to correct answers that were 3's, whereas red points refer to incorrect answers that were 3's. Orange points may be noticed in the performance graphs for Subject 4 and Subject 5. These refer to cases where the participant answered incorrectly when the number presented was not a 3, meaning the participant should have produced a reaction time but did not. The participant either chose incorrectly to not answer or chose to answer correctly but was not able to do so within the trial window. This results in relatively low reaction times in the following trial. None of these instances occurred in the experiments for Subject 1 and Subject 3.

6.2.2 Extracting Features from EEG Data

Two methods were implemented to extract features from the recorded EEG data in this study. In both methods, a sliding window of size 4 trials (4600 milliseconds) with step 2 trials (2300 milliseconds) was used to pull features from temporally aligned slices of both the performance and EEG data. The power spectral densities were then calculated for each slice of EEG data, after which the units of power were converted to units of intensity (dB). In the first method, specific frequencies of interest were chosen from both the beta band (13 - 30 Hz) and the gamma band (31 - 50 Hz). The corresponding intensity at both frequencies of interest were saved as the extracted features from each slice of EEG data. In the second method, both the maximum intensity across the beta band and the maximum intensity across the gamma band were saved as the extracted features from each slice of EEG data. The reason for pursuing two different methods of pulling features from the EEG data is to determine whether pertinent information is contained within the neuronal activity localized around a specific frequency or if all activity within an entire frequency band is more informative.

6.2.3 Average Reaction Time

The first feature of interest that was pulled from the performance data was the average reaction time for each sliding window of 4 trials. The initial proposed hypothesis was that lower levels of engagement would be linked to increased reaction times, meaning that as average reaction times increase it would be expected that signal intensity decreases. Because increased beta activity is assumed to be correlated with higher levels of engagement, this would result in a negative correlation between signal intensity and average reaction time.

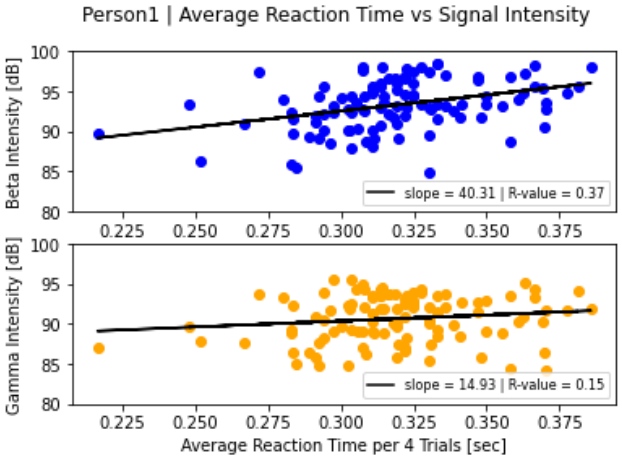

(a) Subject 1 average reaction time versus signal intensities from Method 1.

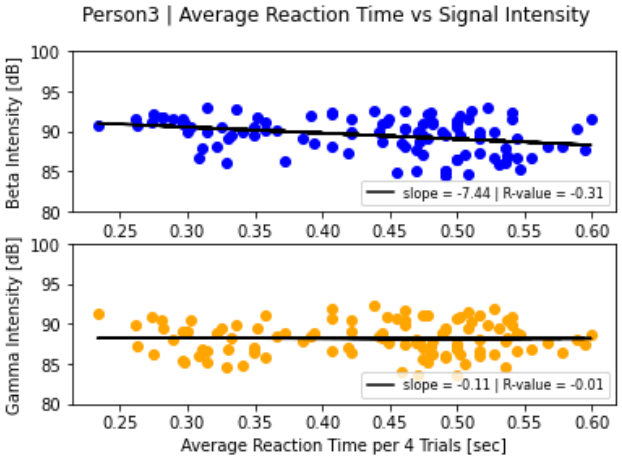

(b) Subject 3 average reaction time versus signal intensities from Method 1.

We plotted the average reaction time against the signal intensity features obtained by implementing Method 1 yielded in Figure 18. In all graphs present in the figure, there appears to be a positive correlation between signal intensity and average reaction time, with beta intensity consistently yielding a higher correlation coefficient than gamma intensity. The only exceptions are in the data produced by Subjects 3 and5, This goes against the original hypothesis that lower average reaction times would be indicative of higher levels of engagement, yielding a negative correla-

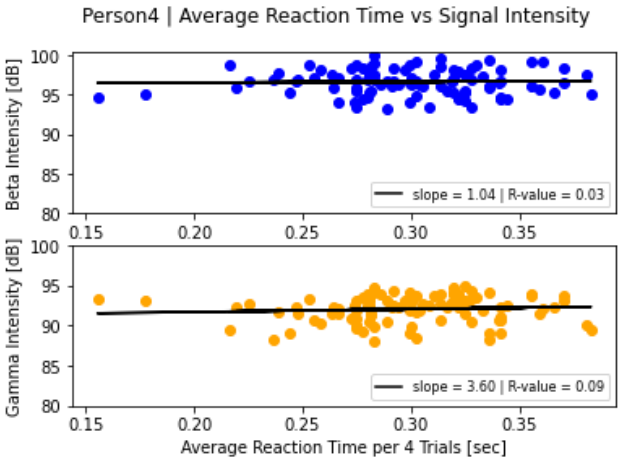

(c) Subject 4 average reaction time versus signal intensities from Method 1.

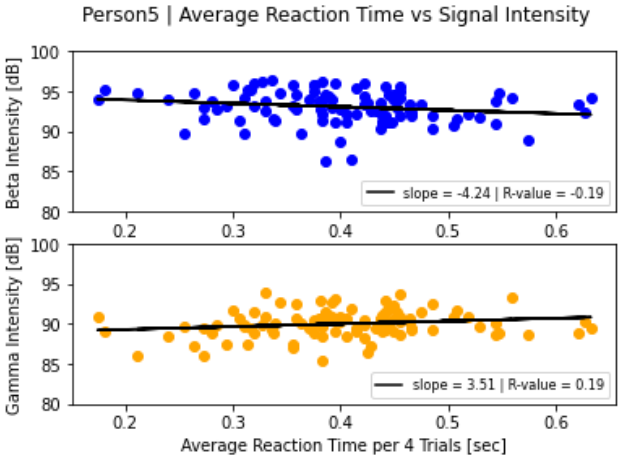

(d) Subject 5 average reaction time versus signal intensities from Method 1.

Figure 18: Average reaction time versus signal intensities from Method 1 for Subject 1, Subject 3, Subject 4, and Subject 5. The horizontal axis represents the average reaction time over a window of trials, and the vertical axis represents signal intensity in units of decibels.

tion coefficient. This supports the claim that higher levels of engagement are linked to slightly increased reaction times because the participant is thinking longer about which action to make.

Figure 19 was produced by plotting the average reaction time against the corresponding signal intensity features obtained through the implementation of Method 2. With the exception of the beta intensity versus average reaction time graphs for Subject 3 and Subject 5, all graphs demonstrate a positive correlation between signal intensity and average reaction time. This supports the same claim as the graphs produced by Method 1, which is that there is an association between lower engagement levels and decreased reaction times. The likely reason for this is that the participant becomes more accustomed to habitually responding faster

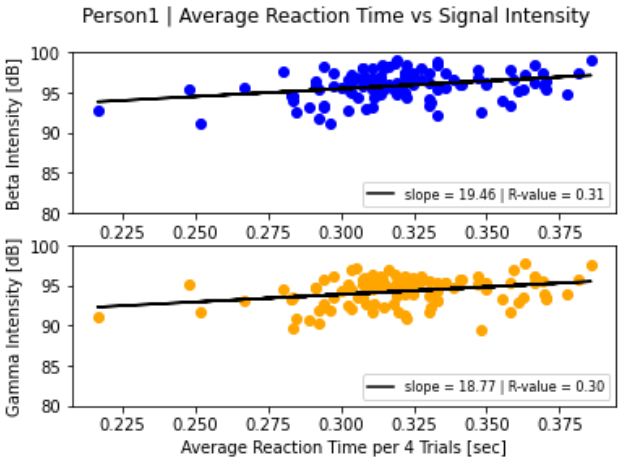

(a) Subject 1 average reaction time versus signal intensities from Method 2.

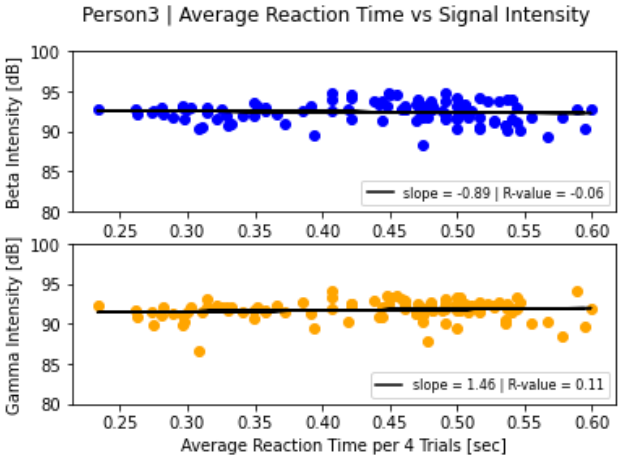

(b) Subject 3 average reaction time versus signal intensities from Method 2.

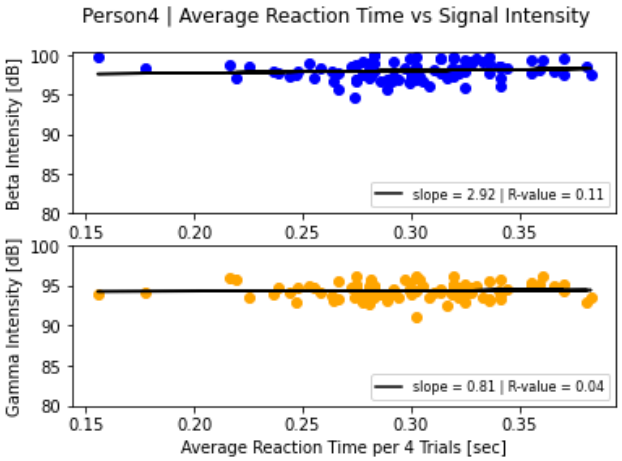

(c) Subject 4 average reaction time versus signal intensities from Method 2.

without regard for the correctness of their answer as they become increasingly disengaged.

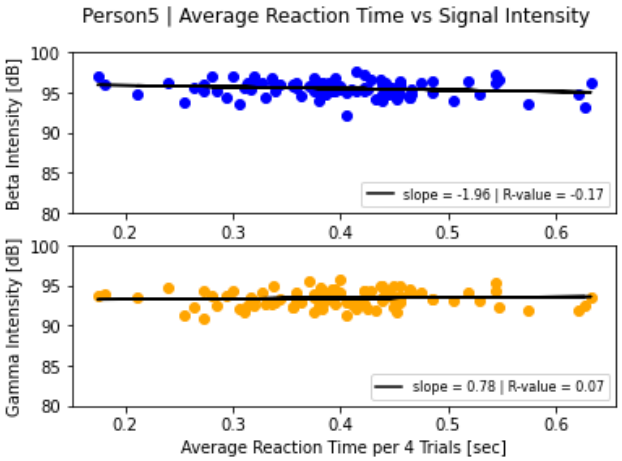

(d) Subject 5 average reaction time versus signal intensities from Method 2.

Figure 19: Average reaction time versus signal intensities from Method 2 for Subject 1, Subject 3, Subject 4, and Subject 5. The horizontal axis represents the average reaction time over a window of trials, and the vertical axis represents signal intensity in units of decibels.

6.2.4 Reaction Time Variance

The second feature extracted from the performance data was the variance in reaction time over each sliding window. Initially, the hypothesis regarding reaction time variance was that there would be a noticeable decrease in both beta and gamma signal intensity as reaction time variance increased. The logic for this hypothesis follows that lower levels of engagement would result in increased reaction time variance, meaning that higher variability in reaction time is indicative of low focus levels.

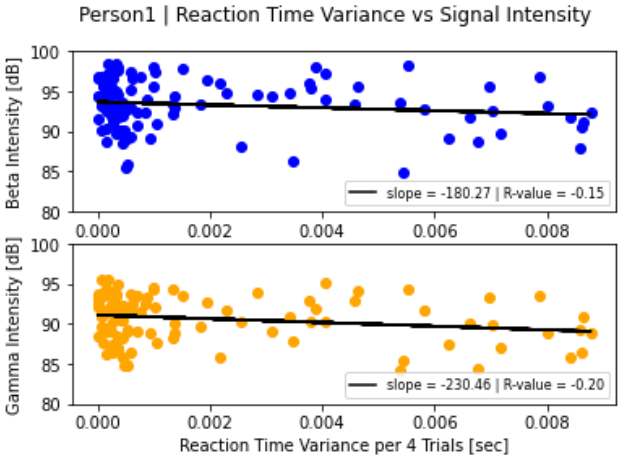

(a) Subject 1 reaction time variance versus signal intensities from Method 1.

Figure 20 displays graphs the resulting from plotting reaction time variance against the signal intensities obtained through implementation of Method 1. All of the graphs,

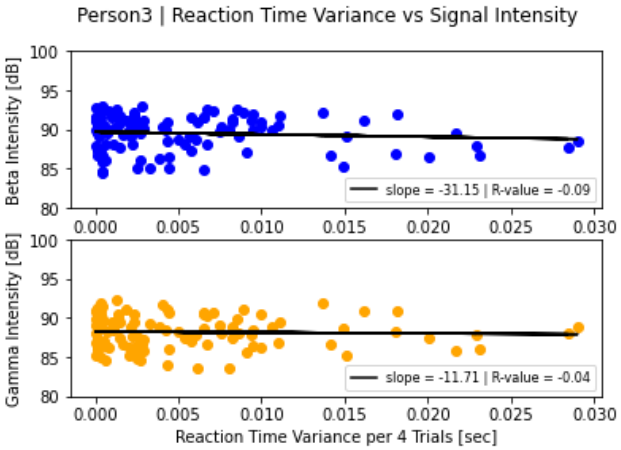

(b) Subject 3 reaction time variance versus signal intensities from Method 1.

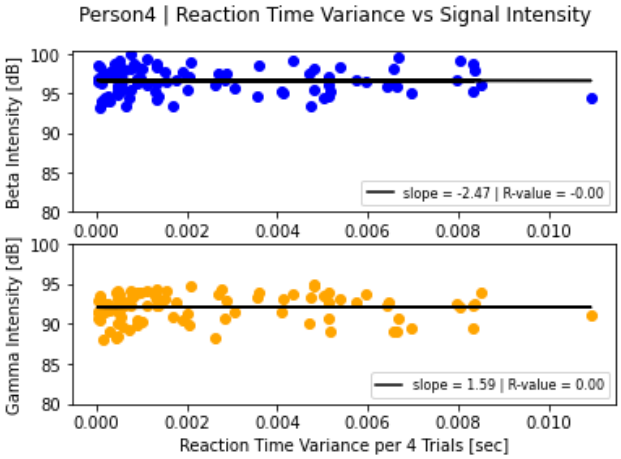

(c) Subject 4 reaction time variance versus signal intensities from Method 1.

with the exception of the beta intensity versus reaction time variance plot for Subject 4 and the gamma intensity versus reaction time variance plot for Subject 5, demonstrate a negative correlation between signal intensity and reaction time variance. This is in alignment with the original hypothesis that signal intensity would increase as reaction time variance decreases, meaning lower variability in reaction time is associated with higher levels of engagement.

Figure 21 illustrates the graphs produced by plotting the signal intensities as obtained through implementation of Method 2 against the variances in reaction time for each sliding window. Excluding the beta intensity against reaction time variance plot for Subject 4, all graphs depict a negative correlation between signal intensity and reaction time variance. Like the plots produced using signal intensities from the first method, this affirms the original hypothesis regarding a negative association between signal intensity and reaction time variance.

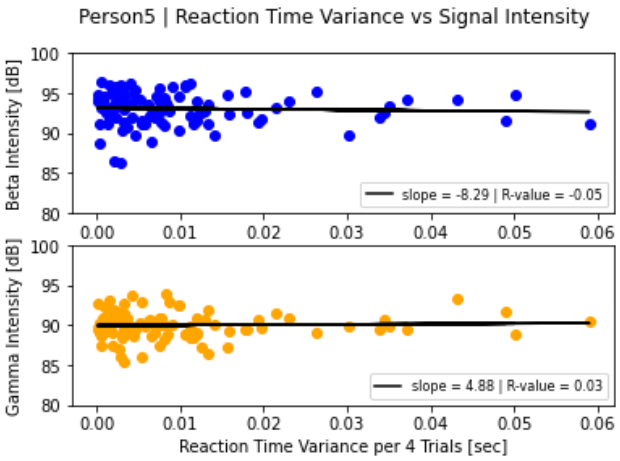

(d) Subject 5 reaction time variance versus signal intensities from Method 1.

Figure 20: Reaction time variance versus signal intensities from Method 1 for Subject 1, Subject 3, Subject 4, and Subject 5. The horizontal axis represents the variance in reaction time over a window of trials, and the vertical axis represents signal intensity in units of decibels.

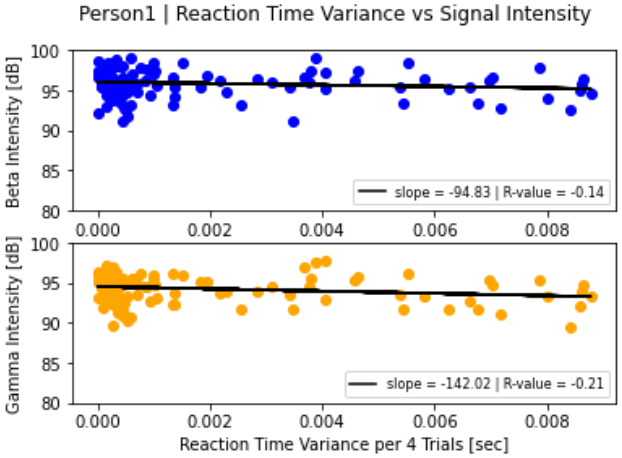

(a) Subject 1 reaction time variance versus signal intensities from Method 2.

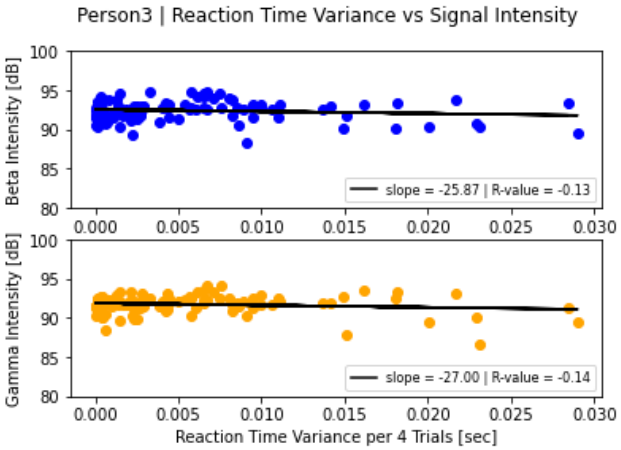

(b) Subject 3 reaction time variance versus signal intensities from Method 2.

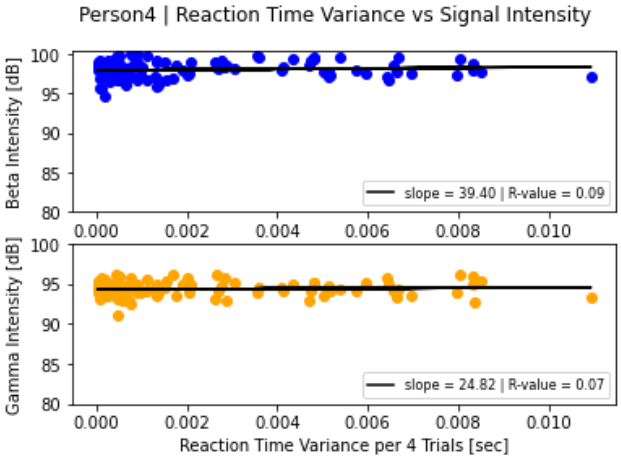

(c) Subject 4 reaction time variance versus signal intensities from Method 2.

6.2.5 Proportion Correct

The third feature derived from the performance data was the proportion of trials answered correctly for each sliding window of 4 trials. Our initial hypothesis involved seeing an increase in the proportion of correct answers per sliding window as beta and gamma signal intensity increases. This comes from the reasoning that higher levels of mental engagement would lead to the participant answering correctly for a larger number of trials per sliding window.

Depicted in Figure 22 are the plots of signal intensities obtained from implementation of the first method versus proportion of correct responses for each sliding window. It may be noted that in none of the participants, except Subject 1, the correlation coefficients of the beta intensity and gamma intensity versus proportion of correct responses plots had the same sign. This means that across all participants, there was only one in which both plots produced either supported the original hypothesis or did not support the original hypothesis.

Figure 23 shows the graphs resulting from implementing Method 2 to obtain signal intensity features then plotting them against the proportion of correct responses for each sliding window. Excluding both plots for Subject 5 and the beta intensity versus proportion of correct responses plot for Subject 4, all other plots demonstrate a positive relationship between signal intensity and proportion of correct responses per sliding window. This supports the original hypothesis claiming that higher response scores are indicative of higher levels of mental engagement.

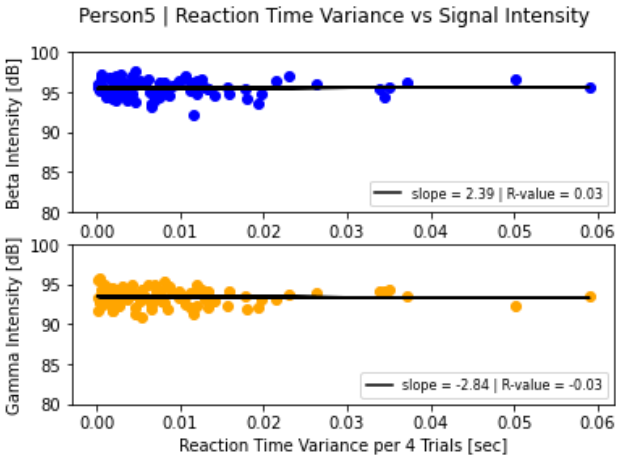

(d) Subject 5 reaction time variance versus signal intensities from Method 2.

Figure 21: Reaction time variance versus signal intensities from Method 2 for Subject 1, Subject 3, Subject 4, and Subject 5. The horizontal axis represents the variance in reaction time over a window of trials, and the vertical axis represents signal intensity in units of decibels.

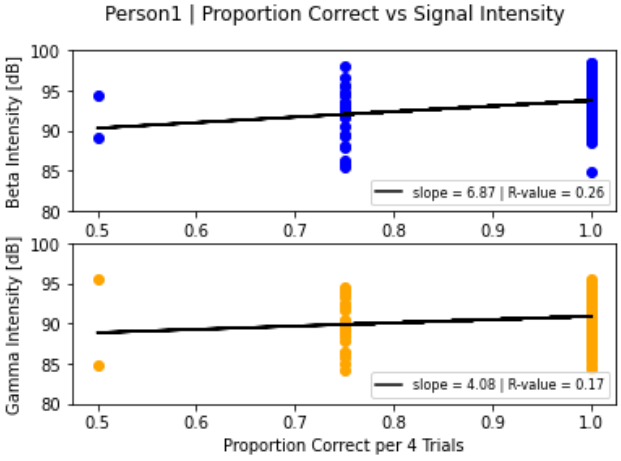

(a) Subject 1 proportion correct versus signal intensities from Method 1.

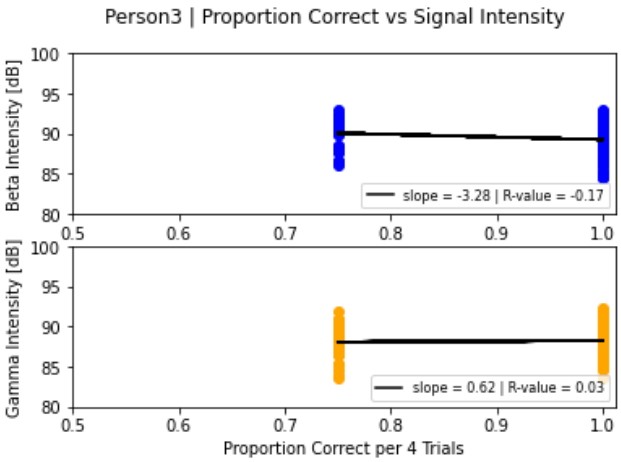

(b) Subject 3 proportion correct versus signal intensities from Method 1.

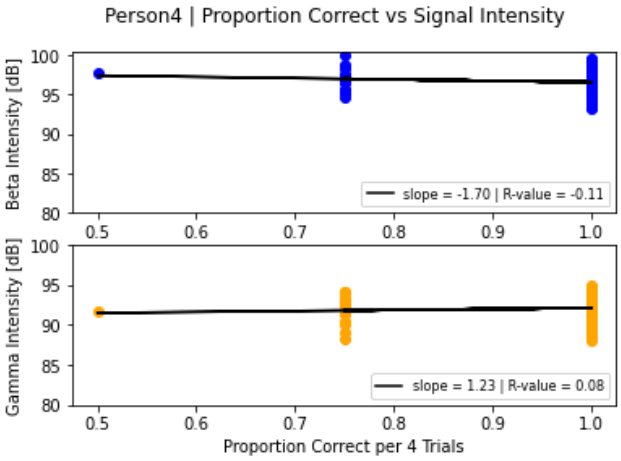

(c) Subject 4 proportion correct versus signal intensities from Method 1.

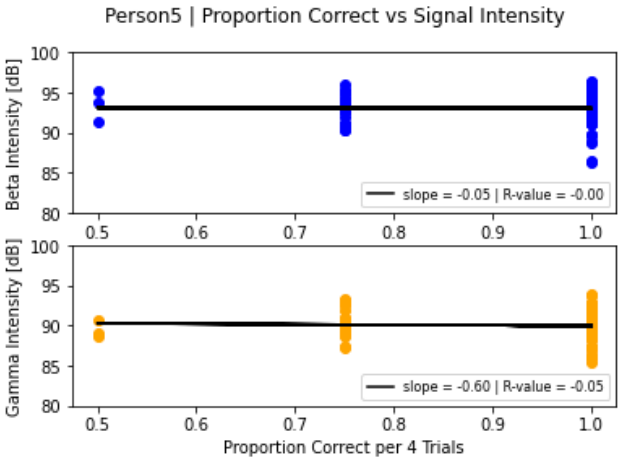

(d) Subject 5 proportion correct versus signal intensities from Method 1.

Figure 22: Proportion correct versus signal intensities from Method 1 for Subject 1, Subject 3, Subject 4, and Subject 5. The horizontal axis represents the proportion of correct responses over a window of trials, and the vertical axis represents signal intensity in units of decibels.

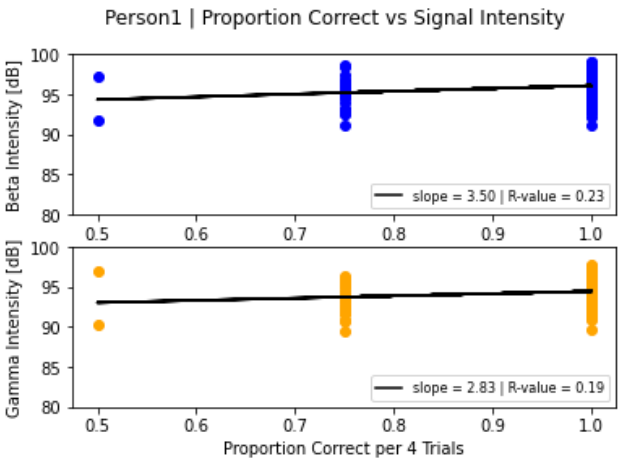

(a) Subject 1 proportion correct versus signal intensities from Method 2.

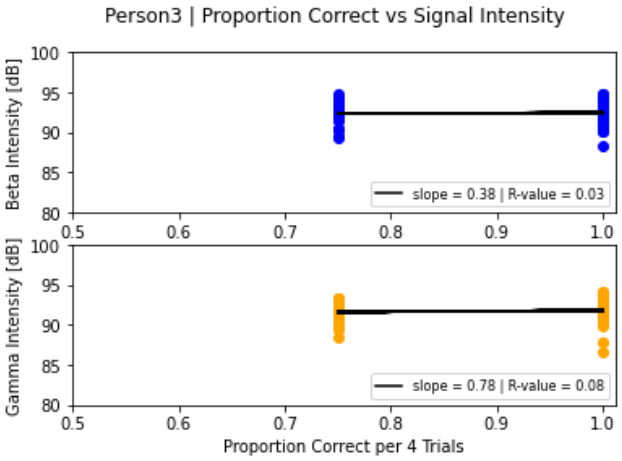

(b) Subject 3 proportion correct versus signal intensities from Method 2.

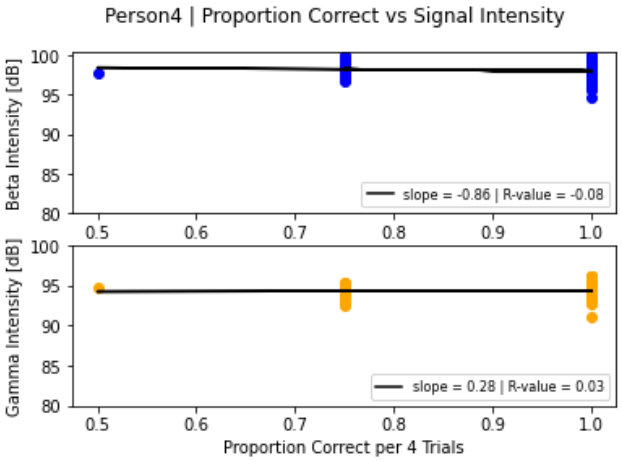

(c) Subject 4 proportion correct versus signal intensities from Method 2.

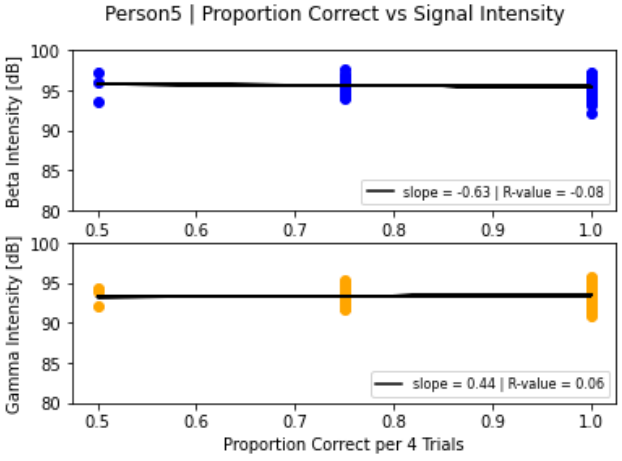

(d) Subject 5 proportion correct versus signal intensities from Method 2.

Figure 23: Proportion correct versus signal intensities from Method 2 for Subject 1, Subject 3, Subject 4, and Subject 5. The horizontal axis represents the proportion of correct responses over a window of trials, and the vertical axis represents signal intensity in units of decibels.

6.2.6 SART Analysis Overview

Deriving signal intensity features using Method 1 did show some correlation with the performance features, proving that there is some relevant information localized around the specific frequencies of interest. However, this information alone does not capture the full picture and therefore deriving signal intensity features using Method 2 proved to be the more informative of the two feature extraction techniques. The least informative of the performance features was the proportion of correct responses for each sliding window, as the correlation coefficients for both the beta intensity versus proportion correct responses plot and the gamma intensity versus proportion correct responses plot were close to zero across all participants except Subject 1 (when using Method 2). However, the most informative of the performance features was average reaction time per sliding window. The plots of beta and gamma signal intensity as obtained through Method 2 versus average reaction time generally demonstrated a positive correlation between the two variables and regression lines with steep slopes, meaning that there is drastic change in information pertaining to beta and gamma signal intensity when there are small increases or decreases in average reaction time.

6.3. Mind-Wandering

The mind wandering experiment paints a picture of user attention by counting mind wandering events, which are defined as the user's type II errors in misspelled word identification (i.e. the user does not identify a misspelled word, incorrectly affirming the null hypothesis that the word is correctly spelled). The times of these events are tracked and recorded alongside EEG data. The following figures show the results of the same mind wandering experiment, run first with the Plux sensor on the F7 electrode, and then with the DSI 24 headset (only showing the spectogram for the F7 electrode to make the most direct comparison possible).

Aside from periodic increases in alpha activity which do not correlate with type II errors, there are no clear trends in the spectogram data for either the Plux or DSI readings. However, the shape of the data itself yields some meaningful results. Firstly, the Plux data contains less artifacts than the DSI data. Additionally, the artifacts in the DSI data are significantly more pronounced and disruptive to the spectogram. This suggests that the Plux sensor may even outperform the DSI headset in terms of data clarity and artifact resistance.

Although we did not find significant changes in EEG activity associated with moments of perceived mind wandering, this experiment did show us that the Plux EEG sensor is capable of providing comparable data to the DSI 24, which is a much more robust and widely used system. This indicates that single (dual if we include reference) electrode EEG sensors can be used in further research.

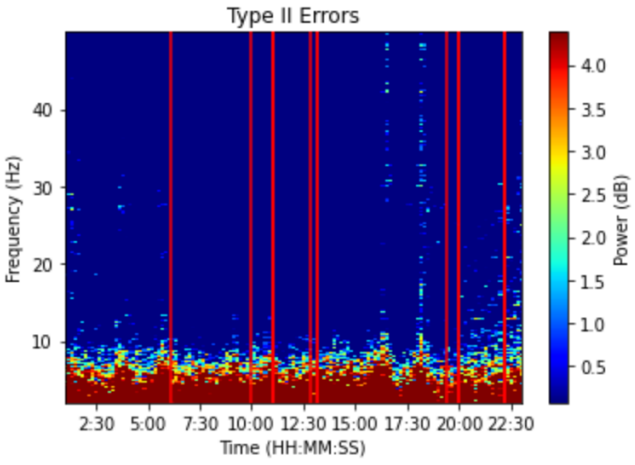

(a) Plux F7 Spectogram

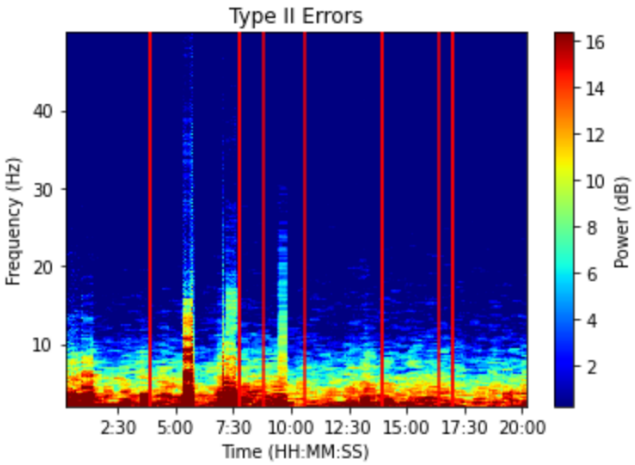

(b) DSI F7 Spectogram

Figure 24: Spectograms collected from Plux and DSI sensors, overlaid by mind wandering events

7. Conclusion

Cognitive neuroscience depends on BCI devices to study neural activity, but modern products – and therefore the research which depends on such tools – are constrained by wearability and modality. Wearable devices are crucial for the future of brain research because they allow for experimentation outside of stationary and delicately pre-positioned activities; there is only so much that can be learned from a subject sitting stationary at a desk, and getting experiments out of the lab is imperative in furthering our understanding of neural processes. The other limitation of modern BCI technology is a lack of multimodality. The ability to collect synchronized multi-sensor data on neural activity unlocks myriad opportunities for analyzing data and understanding the underlying biological processes. Wearable, multimodal BCI devices thus have the potential to redefine the boundaries of cognitive neuroscience. We propose a design for an adhesive, patch-based device with EEG and fNIRS functionality as the solution to these limitations and as a stepping stone for future research using neuroimaging. The device is a disposable patch containing EEG and fNIRS sensors which can be easily attached to a subject. The design is sleek and lightweight, aiming to be as non-intrusive as possible in order to allow for the widest possible range of experimental procedures. The EEG and fNIRS sensors combine high temporal and spatial resolutions respectively to paint a wider and more detailed picture of neural processes than either sensor could create alone. This device is a viable alternative to modern BCI products. Nonetheless, there is still room for improvement upon the prototype going forward. The EEG and fNIRS sensors need to be plugged into a physical hub that is separate from the patch itself. As such, the device is not a true patch since there is an external hub component. Additionally, the physical patch itself has not yet been developed – prototyping and testing have been done solely with sensors and without any unified adhesive casing. These issues do not represent limitations in the design but rather engineering challenges to be pursued in the further development of this device. This device is a stepping stone to a new generation of BCI devices.

7.1. Acknowledgements

We would like to thank Professors Ali Yousefi and Soroush Farzin for mentoring and guiding us throughout this IQP. None of this would have been possible without you. Thank you and we wish you luck and success in your future research.

References

[1] Dsi 24.

[2] *Electrode 10-20 system*. Engineers Community, Jul 2018.

[3] M. Abtahi, G. Cay, M. J. Saikia, and K. Mankodiya. Designing and testing a wearable, wireless fnirs patch. In *2016 38th Annual International Conference of the IEEE Engineering in Medicine and Biology Society (EMBC)*, pages 6298–6301, 2016.

[4] J. Ahn, Y. Ku, D. Kim, J. Sohn, J.-H. Kim, and H. Kim. Wearable in-the-ear eeg system for ssvep-based brain–computer interface. *Electronics Letters*, 54(7):413–414, 2018.

[5] J. W. Ahn, Y. Ku, and H. C. Kim. A novel wearable eeg and ecg recording system for stress assessment. *Sensors*, 19(9), 2019.

[6] S. Ahn and S. C. Jun. Multi-modal integration of eeg-fnirs for brain-computer interfaces – current limitations and future directions. *Frontiers in Human Neuroscience*, 11, 2017.

[7] S. Ahn, T. Nguyen, H. Jang, J. G. Kim, and S. C. Jun. Exploring neuro-physiological correlates of drivers' mental fatigue caused by sleep deprivation using simultaneous eeg, ecg, and fnirs data. *Frontiers in Human Neuroscience*, 10, 2016.

[8] B. e. a. Amin. The role of eeg in the erroneous diagnosis of epilepsy. *Top Geriatr Rehabi*, 2019.

[9] C. e. a. Barros. Advanced eeg-based learning approaches to predict schizophrenia: Promises and pitfalls. *Artificial intelligence in medicine*, 2021.

[10] B. S. e. a. Batail JM. Eeg neurofeedback research: A fertile ground for psychiatry? *L'Encephale*, 45:245–255, 2019.

[11] A. N. e. a. Belkacem. Investigating different stress-relief methods using electroencephalogram (eeg). *IEEE*, 2020.

[12] S. Beniczky and D. L. Schomer. Electroencephalography: basic biophysical and technological aspects important for clinical applications. *Epileptic Disorders*, 22(6):697–715, 2020.

[13] M. A. Bin Altaf, C. Zhang, and J. Yoo. A 16-channel patient-specific seizure onset and termination detection soc with impedance-adaptive transcranial electrical stimulator. *IEEE Journal of Solid-State Circuits*, 50(11):2728–2740, 2015.

[14] A. P. Buccino, H. O. Keles, and A. Omurtag. Hybrid eeg-fnirs asynchronous brain-computer interface for multiple motor tasks. *PLOS ONE*, 11(1):1–16, 01 2016.

[15] B. Byrom, M. Mc Carthy, P. Schueler, and W. Muehlhausen. Brain monitoring devices in neuroscience clinical research: The potential of remote monitoring using sensors, wearables and mobile devices. *Clinical Pharmacology and Therapeutics*, 104, 03 2018.

[16] A. J. Casson. Wearable eeg and beyond. *Biomedical Engineering Letters*, 9:53–71, 2019.

[17] T. Chabin, D. Gabriel, E. Haffen, T. Moulin, and L. Pazart. Are the new mobile wireless eeg headsets reliable for the evaluation of musical pleasure? *PLOS ONE*, 15(12):1–19, 12 2021.

[18] W.-L. Chen, J. Wagner, N. Heugel, J. Sugar, Y.-W. Lee, L. Conant, M. Malloy, J. Heffernan, B. Quirk, A. Zinos, S. A. Beardsley, R. Prost, and H. T. Whelan. Functional near-infrared spectroscopy and its clinical application in the field of neuroscience: Advances and future directions. *Frontiers in Neuroscience*, 14, 2020.

[19] Y. M. Chi and G. Cauwenberghs. Wireless non-contact eeg/ecg electrodes for body sensor networks. In *2010 International Conference on Body Sensor Networks*, pages 297–301, 2010.

[20] R. e. a. Cox. Analyzing human sleep eeg: A methodological primer with code implementation. *Sleep medicine reviews*, 2020.

[21] D. a. Cunnington. Insomnia: prevalence, consequences and effective treatment. *The Medical journal of Australia*, 2013.

[22] D. Dadebayev, W. W. Goh, and E. X. Tan. Eeg-based emotion recognition: Review of commercial eeg devices and machine learning techniques. *Journal of King Saud University - Computer and Information Sciences*, 2021.

[23] M. de Zambotti, N. Cellini, A. Goldstone, I. Colrain, and F. Baker. Wearable sleep technology in clinical and research settings. *Medicine and Science in Sports and Exercise*, 51, 02 2019.

[24] L. e. a. Fiedler. Single-channel in-ear-eeg detects the focus of auditory attention to concurrent tone streams and mixed speech. *Journal of neural engineering*, 2017.

[25] R. B. Firat. Opening the "black box": Functions of the frontal lobes and their implications for sociology. *Frontiers in Sociology*, 4, 2019.

[26] K. Hill, N. L. Plasticity in early alzheimer's disease: An opportunity for intervention. *Top Geriatr Rehabi*, 2011.

[27] H. Hinrichs, M. Scholz, A. Baum, J. Kam, R. Knight, and H.-J. Heinze. Comparison between a wireless dry electrode eeg system with a conventional wired wet electrode eeg system for clinical applications. *Scientific Reports*, 10, 03 2020.

[28] A. e. a. Horvath. Eeg and erp biomarkers of alzheimer's disease: a critical review. *Frontiers in bioscience*, 23:183–220, 2018.

[29] B. Hu, H. Peng, Q. Zhao, B. Hu, D. Majoe, F. Zheng, and P. Moore. Signal quality assessment model for wearable eeg sensor on prediction of mental stress. *IEEE Transactions on NanoBioscience*, 14(5):553–561, 2015.

[30] R. J. Huster, S. Debener, T. Eichele, and C. S. Herrmann. Methods for simultaneous eeg-fmri: An introductory review. *Journal of Neuroscience*, 32(18):6053–6060, 2012.

[31] G. M. Irimia R. Insomnia, sleep disorders, and neurofeedback. *Biodiversity Data Journal*, 2016.

[32] T. Isotani, H. Tanaka, D. Lehmann, R. Pascual-Marqui, K. Kochi, N. Saito, T. Yagyu, T. Kinoshita, and K. Sasada. Source localization of eeg activity during hypnotically induced anxiety and relaxation. *International journal of psychophysiology : official journal of the International Organization of Psychophysiology*, 41:143–53, 06 2001.

[33] V. Jurcak, D. Tsuzuki, and I. Dan. 10/20, 10/10, and 10/5 systems revisited: Their validity as relative head-surface-based positioning systems. *NeuroImage*, 34(4):1600–1611, 2007.

[34] A. Karandinou and L. Turner. Architecture and neuroscience; what can the eeg recording of brain activity reveal about a walk through everyday spaces? *International Journal of Parallel, Emergent and Distributed Systems*, 32(sup1):S54–S65, 2017.

[35] R. e. a. Katmah. A review on mental stress assessment methods using eeg signals. *Sensors*, 2021.

[36] M. J. Khan, M. J. Hong, and K.-S. Hong. Decoding of four movement directions using hybrid nirs-eeg brain-computer interface. *Frontiers in Human Neuroscience*, 8, 2014.

[37] B. Koo, H.-G. Lee, Y. Nam, H. Kang, C. S. Koh, H.-C. Shin, and S. Choi. A hybrid nirs-eeg system for self-paced brain computer interface with online motor imagery. *Journal of Neuroscience Methods*, 244:26–32, 2015. Brain Computer Interfaces; Tribute to Greg A. Gerhardt.

[38] e. a. Krylova, M. Progressive modulation of resting-state brain activity during neurofeedback of positive-social emotion regulation networks. *Nature reviews*, 11:23363, 2021.

[39] J. S. Kumar and P. Bhuvaneswari. Analysis of electroencephalography (eeg) signals and its categorization–a study. *Procedia Engineering*, 38:2525–2536, 2012. INTERNATIONAL CONFERENCE ON MODELLING OPTIMIZATION AND COMPUTING.

[40] J. LaRocco, M. D. Le, and D.-G. Paeng. A systemic review of available low-cost eeg headsets used for drowsiness detection. *Frontiers in Neuroinformatics*, 14, 2020.

[41] A. Lau-Zhu, M. P. Lau, and G. McLoughlin. Mobile eeg in research on neurodevelopmental disorders: Opportunities and challenges. *Developmental Cognitive Neuroscience*, 36:100635, 2019.

[42] G. Li, B.-L. Lee, and W.-Y. Chung. Smartwatch-based wearable eeg system for driver drowsiness detection. *IEEE Sensors Journal*, 15(12):7169–7180, 2015.

[43] G. a. Liberati. Toward a brain-computer interface for alzheimer's disease patients by combining classical conditioning and brain state classification. *Journal of neural engineering*, 2012.

[44] N.-H. e. a. Liu. Recognizing the degree of human attention using eeg signals from mobile sensors. *Sensors (Basel, Switzerland)*, 2013.

[45] . M. e. a. Markiewcz, R. Evaluation of cognitive deficits in schizophrenia using event-related potentials and rehabilitation influences using eeg biofeedback in patients diagnosed with schizophrenia. *Psychiatria polska*, 2019.

[46] H. Morioka, A. Kanemura, S. Morimoto, T. Yoshioka, S. Oba, M. Kawanabe, and S. Ishii. Decoding spatial attention by using cortical currents estimated from electroencephalography with near-infrared spectroscopy prior information. *NeuroImage*, 90:128–139, 2014.

[47] T. Nakamura, V. Goverdovsky, M. J. Morrell, and D. P. Mandic. Automatic sleep monitoring using ear-eeg. *IEEE Journal of Translational Engineering in Health and Medicine*, 5:1–8, 2017.

[48] T. Nguyen, S. Ahn, H. Jang, S. Jun, and J. Kim. Utilization of a combined eeg/nirs system to predict driver drowsiness. *Scientific Reports*, 7, 03 2017.

[49] P. Pinti, C. Aichelburg, S. Gilbert, A. Hamilton, J. Hirsch, P. Burgess, and I. Tachtsidis. A review on the use of wearable functional near-infrared spectroscopy in naturalistic environments. *Japanese Psychological Research*, 60(4):347–373, 2018.

[50] S. K. Piper, A. Krueger, S. P. Koch, J. Mehnert, C. Habermehl, J. Steinbrink, H. Obrig, and C. H. Schmitz. A wearable multi-channel fnirs system for brain imaging in freely moving subjects. *NeuroImage*, 85:64–71, 2014. Celebrating 20 Years of Functional Near Infrared Spectroscopy (fNIRS).

[51] C. J. Price. The evolution of cognitive models: From neuropsychology to neuroimaging and back. *Cortex*, 107:37–49, 2018. In Memory of Professor Glyn Humphreys.

[52] F. Putze, S. Hesslinger, C.-Y. Tse, Y. Huang, C. Herff, C. Guan, and T. Schultz. Hybrid fnirs-eeg based classification of auditory and visual perception processes. *Frontiers in Neuroscience*, 8, 2014.

[53] K. e. a. Rosenow. Non-invasive eeg evaluation in epilepsy diagnosis. *Expert review of neurotherapeutics*, 2015.

[54] M. J. Saikia and K. Mankodiya. A wireless fnirs patch with short-channel regression to improve detection of hemodynamic response of brain. In *2018 International Conference on Electrical, Electronics, Communication, Computer, and Optimization Techniques (ICEECCOT)*, pages 90–96, 2018.

[55] H. Scott, L. Lack, and N. Lovato. A systematic review of the accuracy of sleep wearable devices for estimating sleep onset. *Sleep Medicine Reviews*, 49:101227, 2020.

[56] T. Sheerman-Chase. Eeg brain scan, Oct 2012.

[57] R. e. a. Sitaram. Closed-loop brain training: the science of neurofeedback. *Nature reviews*, 18:86–100, 2017.

[58] T. J. Sullivan, S. R. Deiss, and G. Cauwenberghs. A low-noise, non-contact eeg/ecg sensor. In *2007 IEEE Biomedical Circuits and Systems Conference*, pages 154–157, 2007.

[59] T. Surmeli, A. Ertem, E. Eralp, and I. H. Kos. Schizophrenia and the efficacy of qeeg-guided neurofeedback treatment: A clinical case series. *Clinical EEG and Neuroscience*, 43(2):133–144, 2012. PMID: 22715481.

[60] S. e. a. Thijs. Epilepsy in adults. *Lancet*, 2019.

[61] Y. Tomita, F.-B. Vialatte, G. Dreyfus, Y. Mitsukura, H. Bakardjian, and A. Cichocki. Bimodal bci using simultaneously nirs and eeg. *IEEE Transactions on Biomedical Engineering*, 61(4):1274–1284, 2014.

[62] J. Tremblay, E. Martínez-Montes, P. Vannasing, D. K. Nguyen, M. Sawan, F. Lepore, and A. Gallagher. Comparison of source localization techniques in diffuse optical tomography for fnirs application using a realistic head model. *Biomed. Opt. Express*, 9(7):2994–3016, Jul 2018.

[63] M. Treviño, X. Zhu, Y. Y. Lu, L. S. Scheuer, E. Passell, G. C. Huang, L. T. Germine, and T. S. Horowitz. How do we measure attention? using factor analysis to establish construct validity of neuropsychological tests. *Cognitive Research: Principles and Implications*, 6(51), 2021.

[64] F. Tsow, A. Kumar, S. H. Hosseini, and A. Bowden. A low-cost, wearable, do-it-yourself functional near-infrared spectroscopy (diy-fnirs) headband. *HardwareX*, 10:e00204, 2021.

[65] J. Uchitel, E. E. Vidal-Rosas, R. J. Cooper, and H. Zhao. Wearable, integrated eeg–fnirs technologies: A review. *Sensors*, 21(18), 2021.

[66] A. von Lühmann and K.-R. Müller. Why build an integrated eeg-nirs? about the advantages of hybrid bio-acquisition hardware. In *2017 39th Annual International Conference of the IEEE Engineering in Medicine and Biology Society (EMBC)*, pages 4475–4478, 2017.

[67] L. Vézard, P. Legrand, M. Chavent, F. Faïta-Aïnseba, and L. Trujillo. Eeg classification for the detection of mental states. *Applied Soft Computing*, 32:113–131, 2015.

[68] S. M. Young. *Overview of EEG, Electrode Placement, and Montages. In: Absolute Epilepsy and EEG Rotation Review*. Springer, Cham, 2019.

[69] J. Zhang. Secrets of the brain: An introduction to the brain anatomical structure and biological function. *IFM Lab Tutorial Series*, 2019.

[70] W. e. a. Zhang. Real-time control of a video game using eye movements and two temporal eeg sensors. *Computational intelligence and neuroscience*, 2015.

[71] G. Zimeo Morais, J. Balardin, and J. Sato. Fnirs optodes' location decider (fold): A toolbox for probe arrangement guided by brain regions-of-interest. *Scientific Reports*, 8, 02 2018.